

Supradetachment basins in necking domains of rifted margins: Insights from the Norwegian Sea

Jhon M. Muñoz-Barrera  | Atle Rotevatn  | Robert L. Gawthorpe  | Gijs Henstra  | Thomas B. Kristensen 

Department of Earth Science,
University of Bergen, Bergen, Norway

Correspondence

Jhon M. Muñoz-Barrera, University of Bergen, Realfagbygget, Allégaten 41, 5007, Bergen, Norway.
Email: jhon.munoz@uib.no

Present address

Gijs Henstra, Aker BP, Oksenøyveien 10, Lysaker, 1366, Norway
Thomas B. Kristensen, Equinor, Sandsliveien 90, Sandsli, 5254, Norway

Funding information

ConocoPhillips; Norges Forskningsråd; Tullow Oil; Neptune Energy; Equinor; DNO; Aker BP

Abstract

Supradetachment basins at passive rifted margins are a key witness of major continental extension, and they may preserve a record from which the amount and rates of extension and metamorphic core complex exhumation may be reconstructed. These basins have mainly been recognised in back-arc and orogenic collapse settings, with few examples from rifted margins. Using 2D and 3D seismic reflection, wellbore, and gravity anomaly data, we here characterise the three-dimensional structural and tectonosedimentary evolution of a spoon-shaped supradetachment basin that was formed in the necking domain of a rifted margin, at the southern limit of the Møre and Vøring segments of the Norwegian rifted margin. The basin, with an areal extent of ca. 2400 km², and a landward-rotated syn-tectonic succession up to ca. 30 km thick (true stratigraphic thickness), is separated from footwall continental margin core complex basement culminations by major large-offset (>30 km) normal fault complexes characterised by a cross-sectional geometry whereby an upper, steeper part of the fault gives way to a low-angle detachment fault at depth. These fault complexes are associated with a tectonic thinning of the continental crust to ca. 11 km, compared with a crustal thickness of ca. 27 km in the proximal domain. The basin is filled by a succession of pre-, syn- and post-tectonic deposits, that accumulated over time as the basin evolved over a series of rift- and detachment faulting events. The 30 km thick syn-tectonic succession reflects deposition during two separate rifting events, which are disconnected by deposits reflecting a relative short period of tectonic quiescence. The results are discussed in light of examples of supradetachment basins on other rifted margins globally, as well as in the context of the evolution of the Norwegian margin overall.

KEYWORDS

fracture zone, high- β normal faults, low-angle normal faults, multiphase rifting, passive margins

This is an open access article under the terms of the Creative Commons Attribution-NonCommercial License, which permits use, distribution and reproduction in any medium, provided the original work is properly cited and is not used for commercial purposes.

© 2021 The Authors. *Basin Research* published by International Association of Sedimentologists and European Association of Geoscientists and Engineers and John Wiley & Sons Ltd.

1 | INTRODUCTION

Supradetachment basins are basins formed in the hanging wall of low-angle ($<30^\circ$), high-displacement (>5 km) normal faults, which also exhume rocks from below the brittle-ductile transition in their footwalls due to major continental extension (Figure 1; Friedmann & Burbank, 1995; Lister et al., 1986; Peron-Pinvidic et al., 2013; Platt et al., 2014; Whitney et al., 2013). The footwall of these high-displacement faults, also referred to as the lower plate (Wernicke, 1981), typically shows a domal geometry (metamorphic core complex), whereas their hanging wall, also called the upper plate (Wernicke, 1981), is composed of rocks from the upper continental crust, low-grade metamorphic rocks and syn-tectonic supradetachment basins (Davis, 1980). The study of syn-tectonic deposits in supradetachment basins is essential to determine the amount of extension and rates of footwall exhumation associated with major-continental extension (Asti et al., 2018). Supradetachment basins typically present four characteristics: (i) thick syn-tectonic deposits up to tens of kilometres thick, with strong landward stratal rotation (up to 50°) above a low-angle, high-displacement normal fault (Friedmann & Burbank, 1995; Jongepier et al., 1996), (ii) four sources of sediments: footwall-derived, hanging wall derived, axially derived, and transfer zones derived (*sensu* Gawthorpe et al., 1994), all of which are active during and following the rifting episode (Osmundsen et al., 1998; Ribes et al., 2019), (iii) two types of sedimentary contacts, i.e., tectonic and stratigraphic (Figure 1; Ribes et al., 2019; Vetti & Fossen, 2012; Whitney et al., 2013), and (iv) a high palaeo-geothermal gradient (150 and 180 mW/m²) of the basal syn-tectonic units during and after deposition (Whitney et al., 2013). Few studies, however, provide insights into the three-dimensional geometry and evolution of such basins (notable exceptions include Osmundsen et al., 1998; Vetti & Fossen, 2012).

The three-dimensional geometry of supradetachment basins is controlled by (i) the detachment fault geometry, (ii) exhumation of middle to lower crustal rocks in the footwall or (iii) extension and processes that develop the distal domains of rifted margins (Fillmore et al., 1994; Friedmann & Burbank, 1995; Lymer et al., 2019; Osmundsen & Péron-Pinvidic, 2018; Peron-Pinvidic et al., 2013; Wiest et al., 2019). Figure 1 outlines the geometry of four idealised end-members of supradetachment basin types and their location in a rifted margin. Fillmore et al. (1994) propose the term “breakaway-type basin” (Figure 1b) for supradetachment basins generated during the evolution of metamorphic core complexes with a major axis perpendicular to the extension direction (also called “b-type” dome *sensu* Jolivet et al., 2004). Breakaway-type basins have been recognised in areas of orogenic collapse, back-arc settings and necking domains of rifted margins

Highlights

- Seismic reflection and wellbore data is used to investigate the 3D geometry of supra-detachment basins
- We focus on the necking domain of rifted margins, where thick continental crust is thinned
- The tectonostratigraphic evolution of spoon-shaped supra-detachment basin is elucidated
- Supradetachment basins form by high-displacement, low-angle normal faulting during multiphase rifting

(Figure 1a,b,d; e.g., Chéry, 2001; Dermircioğlu et al., 2010; Fillmore et al., 1994; Forshee & Yin, 1995; Friedmann & Burbank, 1995; Jongepier et al., 1996; Kapp et al., 2008; McClaghry & Gaylord, 2005; Miller & Pavlis, 2005; Osmundsen & Péron-Pinvidic, 2018; Seranne & Seguret, 1987; Woodruff et al., 2013). Seranne and Seguret (1987) suggested the term “spoon-shaped basin” (Figure 1c) for supradetachment basins located between two metamorphic core complexes with major axes parallel to the extension direction (also termed “a-type” domes *sensu* Jolivet et al., 2004). Vetti and Fossen (2012) introduce the term “ramp basin” (Figure 1c) for bowl-shaped supradetachment basins caused by a flat-ramp-flat geometry of the detachment faults. Spoon-shaped and ramp basins have been associated with areas of orogenic collapse and back-arc structural settings (Osmundsen et al., 1998; Seranne & Seguret, 1987; Vetti & Fossen, 2012). Tugend et al. (2014) use the term “hyperextended sag basin” to describe a supradetachment basin, with sub-parallel to parallel syn-tectonic strata in the distal domain of hyperextended rifted margins (Figure 1a,f; Lymer et al., 2019; Peron-Pinvidic et al., 2013). Only Jongepier et al. (1996) and Osmundsen and Péron-Pinvidic (2018), however, describe a “breakaway” supradetachment basin in a necking domain, the Slørebotn Subbasin, Norway.

In this paper, we elucidate, for the first time, the three-dimensional geometry of a spoon-shaped supradetachment basin developed in the necking domain of a rifted margin (Figure 1a,e), which is the domain where the continental crust is thinned from ca. 30 to 10 km. We integrate interpretation of 3D and 2D reflection seismic and well data, with the interpretation of gravity data (Olesen, Ebbing, et al., 2010) and the Moho (Maystrenko et al., 2018) from the southeast limit of the Møre and Vøring segments of the Norwegian rifted margin (Figure 2), specifically in the area where the Klakk Fault Complex (Klakk FC) and Møre-Trøndelag Fault Complex (MTFC) intersect. We describe the geometry, structure, and evolution

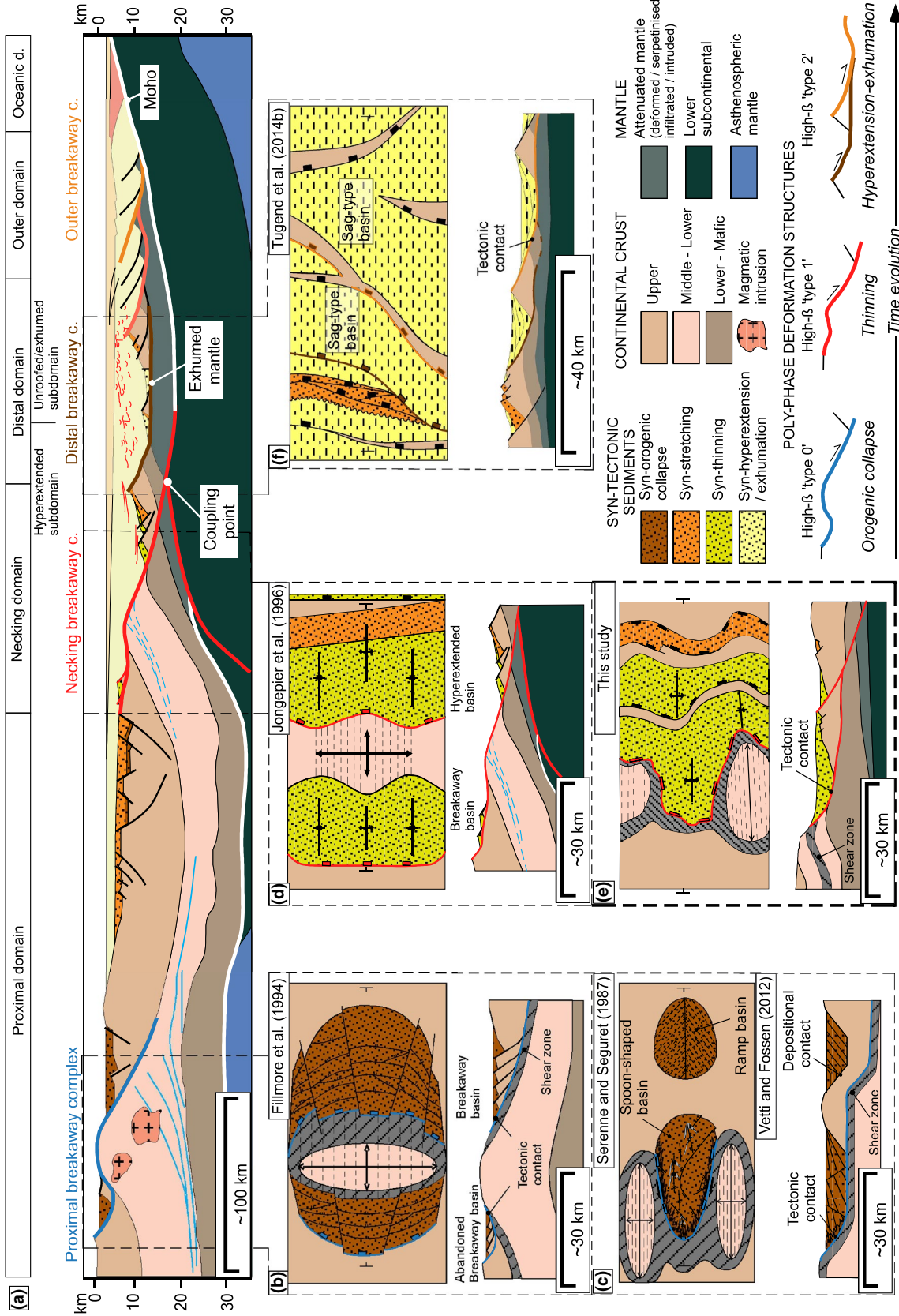


FIGURE 1 Idealised model of supradetachment basins in different tectonic settings. (a) Cross-section of a rifted margin (modified from Masini et al., 2012; Péron-Pinvidic et al., 2013; Osmundsen & Péron-Pinvidic, 2018). (b) Breakaway basin model by Fillmore et al. (1994) developed in a continental crust > 35 km thick. Map view adapted from Asti et al. (2018). (c) Spoon-shaped basin model by Serenne and Seguret (1987) and ramp basin by Vetti and Fossen (2012) developed in a continental crust > 35 km thick. Map view adapted from Vetti and Fossen (2012) and Osmundsen and Andersen (2001). (d) Breakaway basin model in necking domains of rifted margins adapted from Jongepier et al. (1996). Map view adapted from Osmundsen and Péron-Pinvidic (2018). (e) Spoon-shaped supradetachment basin in necking domains of rifted margins (This work). (f) Sag-type basins by Tugend et al. (2014). Map view adapted from Péron-Pinvidic et al. (2013)

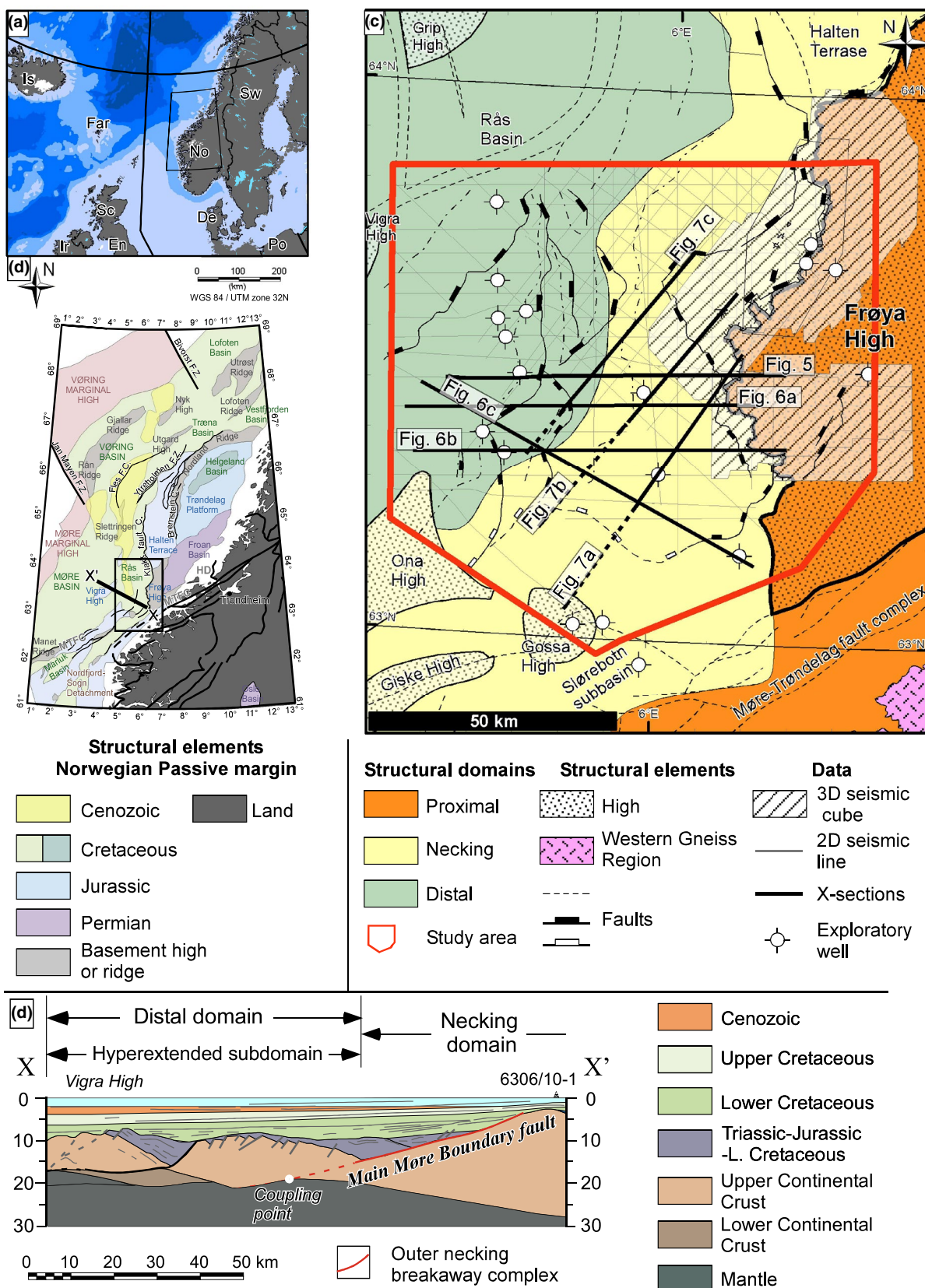


FIGURE 2 Location of study area. (a) General map of the study area. No, Norway. (b) Map of the Norwegian passive margin; adapted from Osmundsen et al. (2016). (c) Zoom study area, limits between Møre and Vøring basin. Structural elements updated from Blystad et al. (1995), and gravity anomaly values adapted from Olesen, Gellein, et al. (2010). (d) Cross-section in the study area, adapted from Osmundsen et al. (2016), Location of cross-section in Figure 2b

of the basin, and discuss the factors that controlled its development. Our findings provide insights that are applicable to supradetachment basins in similar settings globally and have implications for understanding the evolution of rifted margins.

2 | GEOLOGICAL SETTING

The supradetachment basin studied in this paper is located in the intersection between the Klakk FC, MTFC and Jan Mayen Lineament, along the southern limit of the Møre and Vøring segments of the Norwegian rifted margin (Figures 2 and 3). Following the Caledonian orogeny in Silurian to Devonian times (Corfu et al., 2014; Gee et al., 2013), the study area has undergone a long-lived, complex history of protracted extension, from post-orogenic collapse in Devonian times (Andersen & Jamtveit, 1990; Fossen, 2010), through episodic rifting throughout the Palaeozoic and Mesozoic (Faleide et al., 2008; Peron-Pinvidic et al., 2013; Tsikalas et al., 2012), culminating in the opening of the NE Atlantic in late Palaeocene-early Eocene times (Figures 2 and 3; Faleide et al., 2008; Gernigon et al., 2009, 2020; Peron-Pinvidic et al., 2013; Péron-Pinvidic & Osmundsen, 2018; Tsikalas et al., 2012; Zastrozhnov et al., 2018). Inheritance structures such as shear zones, faults and lithology controlled the evolution of the margin during the first two rift deformation phases, i.e., the “stretching” and “thinning” phases (*sensu* Peron-Pinvidic et al., 2013), in the Norwegian margin (e.g., Mjelde et al., 2009, 2013; Muñoz-Barrera et al., 2020; Osmundsen et al., 2005, 2021; Péron-Pinvidic et al., 2020; Zastrozhnov et al., 2018). In this paper, we use the terms of stretching, thinning, hyperextension-exhumation phases defined by Péron-Pinvidic et al. (2013). Stretching phase corresponds to the first-rift phase where the deformation focusses on a thick continental crust (>30 km). Thinning phase is the second-rift phase, where the deformation thins the continental crust from 30 to 10 km thick. Hyperextension-exhumation phase corresponds to the third-rift phase where deformation occurs on a continental crust >10 km thick.

2.1 | Structural configuration of the study area

The Klakk FC and MTFC form the necking domain in this part of the Norwegian rifted margin (Peron-Pinvidic et al., 2013). The down-to-the-west Klakk FC is ca. 270 km long and has a N-S strike and zig-zag plan-view geometry (Figure 2c). The Klakk FC separates the Frøya High-Sklinna

Ridge (in its footwall) from the Rås Basin (in its hanging wall; Blystad et al., 1995; Muñoz-Barrera et al., 2020). This fault system features high-displacement (>5 km) faults, with listric to planar cross-sectional geometries (Muñoz-Barrera et al., 2020; Osmundsen & Péron-Pinvidic, 2018; Peron-Pinvidic et al., 2013). The down-to-the-northwest MTFC strikes NE-SW is ca. 750 km long and is composed of several fault segments in a zone ca. 80 km wide (Figure 2b,d; Gabrielsen et al., 1999; Nasuti et al., 2012). The MTFC separates the Gossa High (in its footwall) from the Rås basin (in its hanging wall). The MTFC began with sinistral transtensional movements during the Devonian (Braathen et al., 2000), and followed by reactivation with normal to dextral transtensional movements during the Triassic, Jurassic and Late Cretaceous-Cenozoic (Mørk & Johnsen, 2005; Mørk & Stiberg, 2003; Redfield et al., 2005; Sommaruga & Bøe, 2002). The high displacement of the segments that compose the Klakk FC and MTFC produced continental margin core complexes on the Gossa High and the north-western part of the central structural salient on the Frøya High (Muñoz-Barrera et al., 2020; Osmundsen & Péron-Pinvidic, 2018).

The Jan Mayen Lineament limits the study area to the north within the Rås Basin (Figure 2c). The Jan Mayen Lineament embodies the SE-ward extension of the NW-SE-trending Jan Mayen Fracture Zone (Figure 2b; Ebbing & Olesen, 2011; Gernigon et al., 2009; Maystrenko et al., 2018; Zastrozhnov et al., 2018). Gernigon et al. (2009) identified that the Jan Mayen Fracture Zone has acted as a long-lived magmatic corridor for melts in the lithosphere. Mjelde et al. (2016) associate the Jan Mayen Fracture Zone and Jan Mayen Lineament to an inherited crustal tear fault, which separated different dip domains of the subducted Baltica plate and may be responsible for the different structural configurations between the Møre and Vøring basins.

2.2 | Stratigraphy of the study area

We extrapolate the stratigraphy below the Upper Cretaceous from wells and published data from the Slørebotn Subbasin (Jongepier et al., 1996), Frøya High, Froan Basin (Müller et al., 2005), Halten Terrace (Bell, Jackson, Elliott, et al., 2014; Ravnås et al., 2014) to the southeast Rås Basin, due of the lack of well penetration in the study area (Figure 3). Baltic granite and gneiss compose the basement on the Frøya High and Gossa High (Figures 2 and 3; Slagstad et al., 2011; boreholes 6306/10-1, 6306/6-1 and 6306/6-2, Norwegian Petroleum Directorate, Factpages, 2000). Several authors have interpreted Pre-Triassic rocks based on seismic reflections data at the Halten Terrace, Froan Basin, Rås Basin and Frøya High

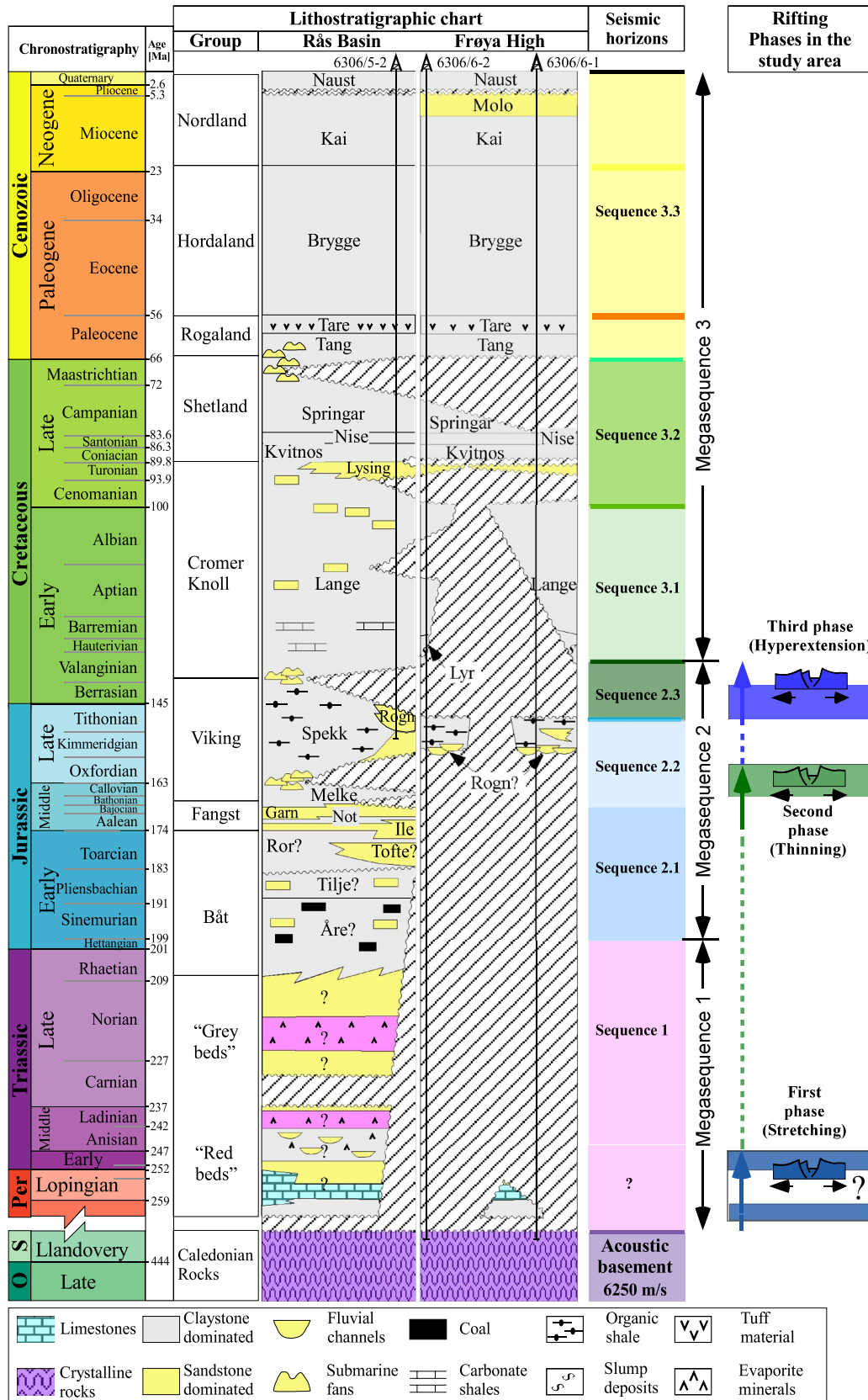


FIGURE 3 Stratigraphic chart of the study area. Lithostratigraphic chart modified from Bell, Jackson, Elliott, et al. (2014) using the information of wells referenced. Tectonic events based on Perón-Pinvidic et al. (2013). Sequence and Mega-sequences interpreted (see text)

(e.g., Blystard et al., 1995; Müller et al., 2005; Osmundsen et al., 2016; Trice et al., 2019; Wilson et al., 2013). These authors argue that Devonian sediments record the Caledonian orogenic collapse phase, whereas Permian to Middle Triassic deposits are associated with the first rift phase or stretching phase (*sensu* Peron-Pinvidic et al., 2013) in the Norwegian Margin (Blystard et al., 1995; Faleide et al., 2008; Müller et al., 2005; Peron-Pinvidic et al., 2013; Tsikalas et al., 2012). Subsequently, the area underwent a tectonically quiescent period during Late Triassic times leading to the deposition of thick beds of evaporites and paralic deposit as reported in wells 6306/6-1, 6407/10-3 and 6407/10-4 on the Frøya High, 6407/9-1 and 6307/1-1S within the Froan Basin, and 6407/7-1S and 6406/11-1S within the southern Halten terrace (Müller et al., 2005; Norwegian Petroleum Directorate, Factpages, 2000).

Jurassic deposits have been reported on the Halten Terrace, the Froan basin, the Frøya High and the Slørebotn Subbasin (Figure 2) as part of the second rift phase (thinning phase; *sensu* Peron-Pinvidic et al., 2013; Borehole 6306/6-1; Dalland et al., 1988; Jongepier et al., 1996; Norwegian Petroleum Directorate, Factpages, 2000; Ravnås et al., 2014). Paralic-to-shallow-marine sandstones and mudstone-rich formations were deposited during Lower to Middle Jurassic on the Halten Terrace during a mild rifting (Ravnås et al., 2014; Figure 3). The climax of the second rift phase, that is, the “thinning” phase (*sensu* Peron-Pinvidic et al., 2013), occurred during the Late Jurassic and is recorded by syn-tectonic fan delta sandstones, shallow-marine sand bodies and deep-water gravity-flow deposits on the southern Halten Terrace, Slørebotn Subbasin and to the west of the Frøya High (Figures 2 and 3; Jongepier et al., 1996; Provan, 1992; Wilson et al., 2015). The second rift phase ended with deposition of the Spekk Formation during the Oxfordian-Berriasian, which capped the majority of the Frøya High (borehole report 6306/6-1 in Norwegian Petroleum Directorate, Factpages, 2000; Dalland et al., 1988). The Base Cretaceous Unconformity (BCU) represents a prominent regional seismic reflection on the Norwegian margin (Osmundsen et al., 2016; Zastrozhnov et al., 2018). In the Frøya High and Gossa High, the BCU separates basement, or, locally, Jurassic deposits, from overlying Cretaceous deposits. Within the Rås Basin and on the Halten Terrace, the BCU is a conformable surface represented by the top of the Spekk Formation (Figure 3; Bell, Jackson, Elliott, et al., 2014; Dalland et al., 1988; Osmundsen et al., 2016).

Lowermost Cretaceous sediments have been reported in the Slørebotn Subbasin in conformable contact with Upper Jurassic deposits, whereas the Lower Cretaceous sediments are missing on the basement highs (Jongepier et al., 1996; Zastrozhnov et al., 2018; boreholes 6205/12-1,

6205/12-2, 6205/3-1R, 6306/10-1, 6306/6-1 and 6306/6-2 in Norwegian Petroleum Directorate, Factpages, 2000). These lowermost Cretaceous deposits represent syn-tectonic “growth” strata accumulated during the third rift phase (Hyperextension, *sensu* Peron-Pinvidic et al., 2013). Lower Cretaceous to Cenozoic marine sediments cover the Norwegian rifted margin in this area representing the post-kinematic phase (Dalland et al., 1988).

3 | DATA AND METHODOLOGY

The data used in this study comprise 17 exploration wells, 60 2D reflection seismic profiles (3511 km in total length) and five 3D reflection seismic volumes (3806 km² total coverage; Figure 2). We integrate these data with the gravity anomaly map of Olesen, Ebbing, et al. (2010) and the geophysical Moho interpretation by Maystrenko et al. (2018). We obtained well-tops, well-paths, velocity data and well reports from the Norwegian National Data Repository for Petroleum data (DISKOS). Further information about subsurface datasets and interpretation, domain conversion, velocity model, and structural restorations, can be found in Supporting Information A to D.

We used the major phases of basin evolution to identify three seismic megasequences (Hubbard, 1988). These megasequences are composed of seismic sequences, which are defined based on (i) the characteristics of their base and top boundaries; (ii) their overall extent and cross-sectional shape; and (iii) the lateral and stratigraphical variations in reflector characteristics and the component seismic facies. These seismic sequences are defined by seismic facies that form our basis for the interpretation of their depositional origin (*sensu* Sangree & Widmier, 1979).

4 | PRESENT STRUCTURAL CONFIGURATION OF THE SUPRASETACHMENT BASIN

A supradetachment basin sits in the hanging wall of two high-displacement (>20 km) listric normal fault complexes, the Klakk FC and the MTFC, which form the bounding faults of the supradetachment basin (Figures 4–7). The depth converted sections show that these fault complexes feature “listric” geometries, whereby and upper, steeper part gives way to a progressively low-angle “detachment” fault at depth (Figures 5–7). These detachment faults are associated with a thinning of the continental crust to ca. 11 km (necking domain), compared with a thickness of ca. 27 km in the proximal domain (Figure 5). The supradetachment basin forms an embayment to the Rås Basin and shows a trough-like geometry in three dimensions. The

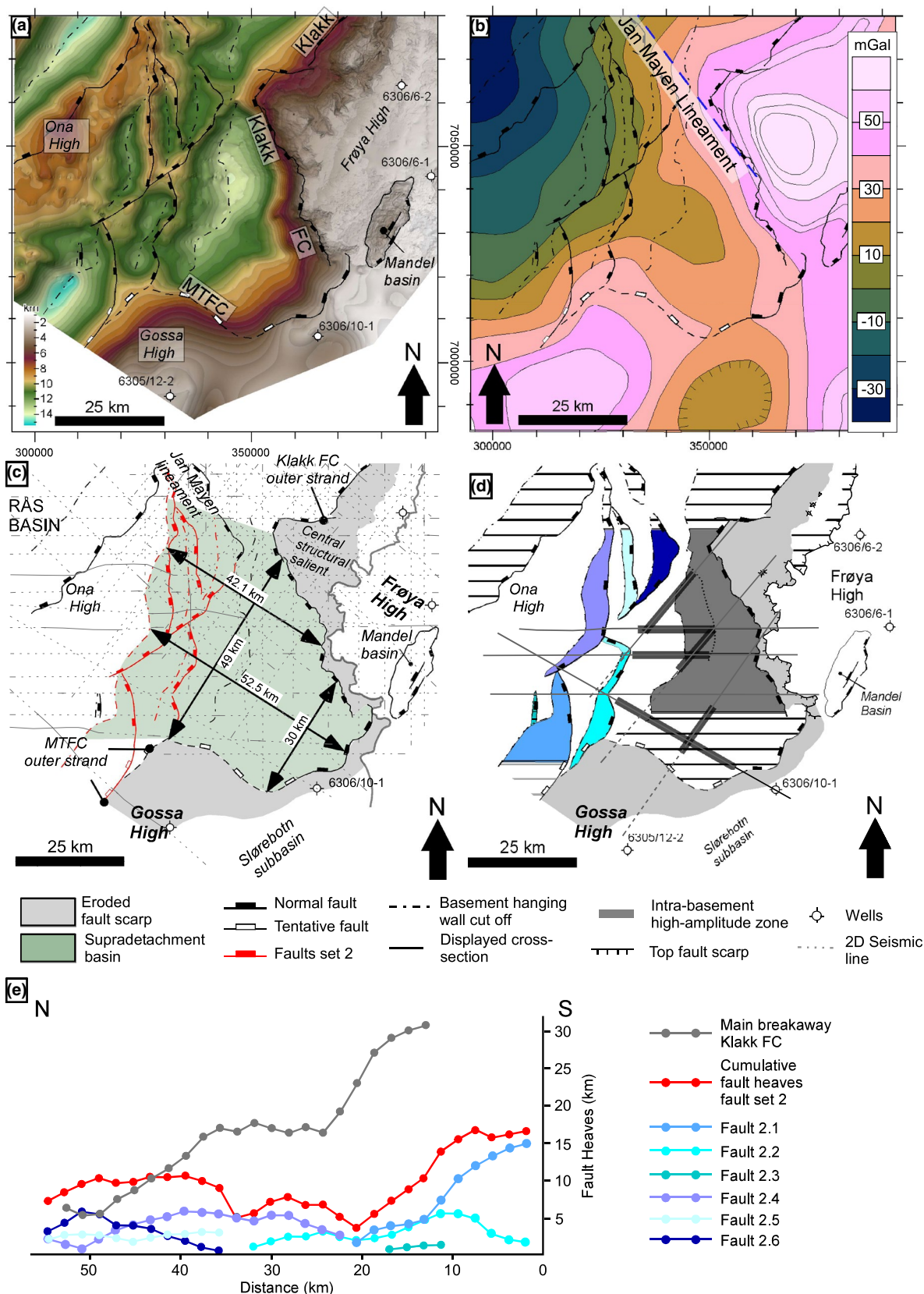


FIGURE 4 Structural configuration of the supradetachment basin at the top of the acoustic basement in the study area. (a) Structural map at the top acoustic basement, (b) gravity anomaly map digitalised from Olesen, Ebbing, et al. (2010), (c) Basin geometry, (d) fault polygons map at top acoustic basement, (e) heave plot at top acoustic basement

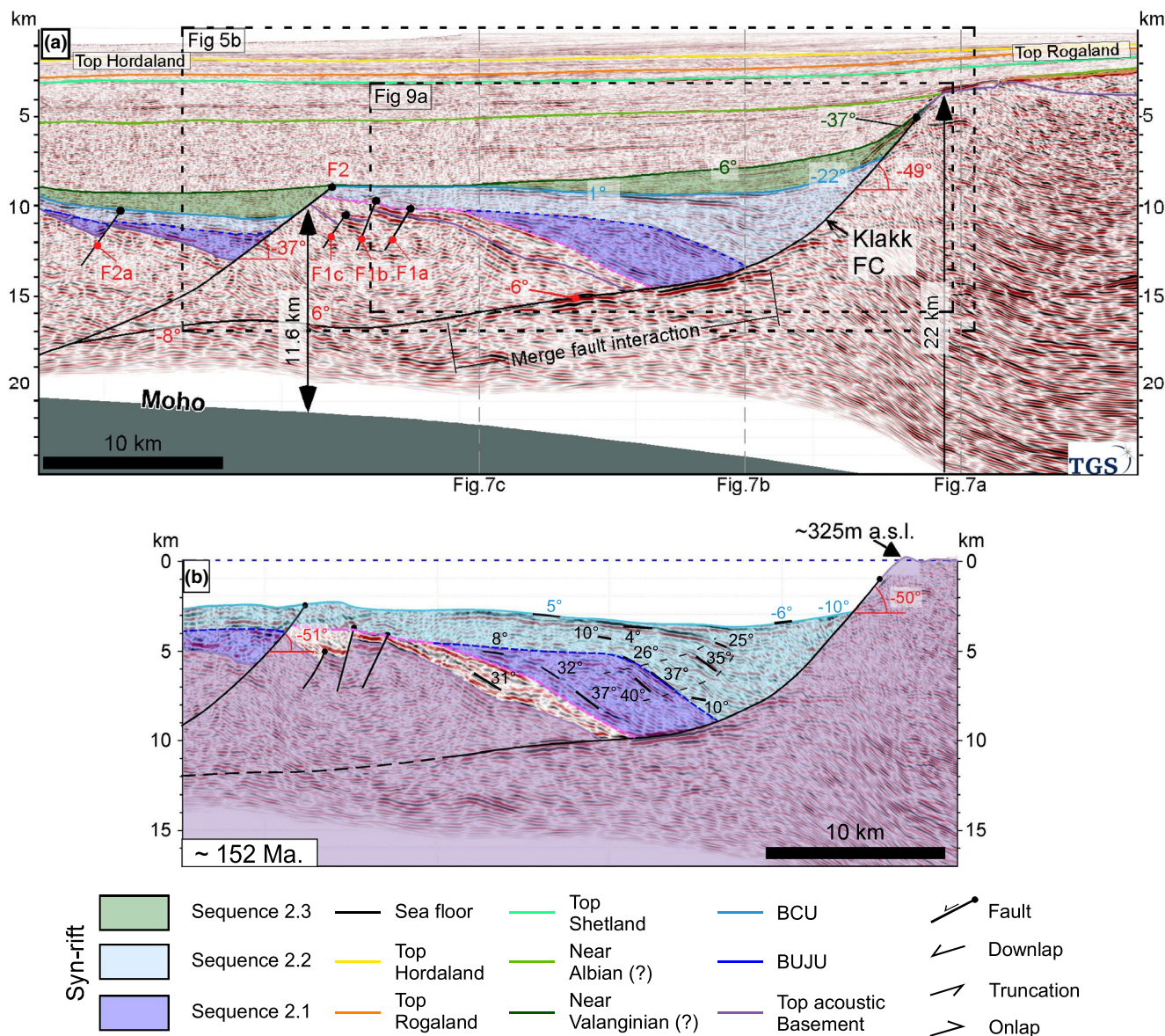


FIGURE 5 Dip cross-section in the northern part of the supradetachment basin. (a) Interpreted section in depth domain. (b) Restoration of line MNR07-7043B back to the late Jurassic period. Moho deep by Maystrenko et al. (2018). Location Figures 2 and 4. Full restored section in Figure S3 (Supporting Information)

basin extends ca. 52.5 km in the dip-parallel direction, with a variable width ranging from ca. 30 km in the southeast to ca. 49 km towards the northwest; the basin is filled with syn-tectonic sediments and is up to ca. 2.5 s TWT thick (ca. 6 km true vertical depth; Figure 4). The sedimentary succession within the basin displays a slope-front geometry with localised fan geometries towards the main bounding faults (Figures 5–7). The stratigraphic succession shows a post-depositional landward rotation from ca. 40° west to ca. 30° east (Figure 5), which produced a cumulated stratigraphic thickness of up to 30 km (Figure 6b).

Although Cretaceous and Cenozoic thermal subsidence tilted the area towards the northwest (Bell, Jackson, Elliott, et al., 2014), the restoration of the section in Figure

5b suggest that the current basin geometry is similar to the geometry during rifting.

4.1 | Bounding faults of the supradetachment basin

The Klakk FC shows two NW–SE-striking faults segments connected via a N–S-striking fault generating a zigzag geometry in plan-view (Figure 4). The southern segment is ca. 14 km long, and its heave decreases northward from ca. 30 to 18 km (Figure 4 and Table 1). The central segment is ca. 10 km long and has a heave of ca. 17 km, whereas, the northern segment is ca. 23 km long, and its

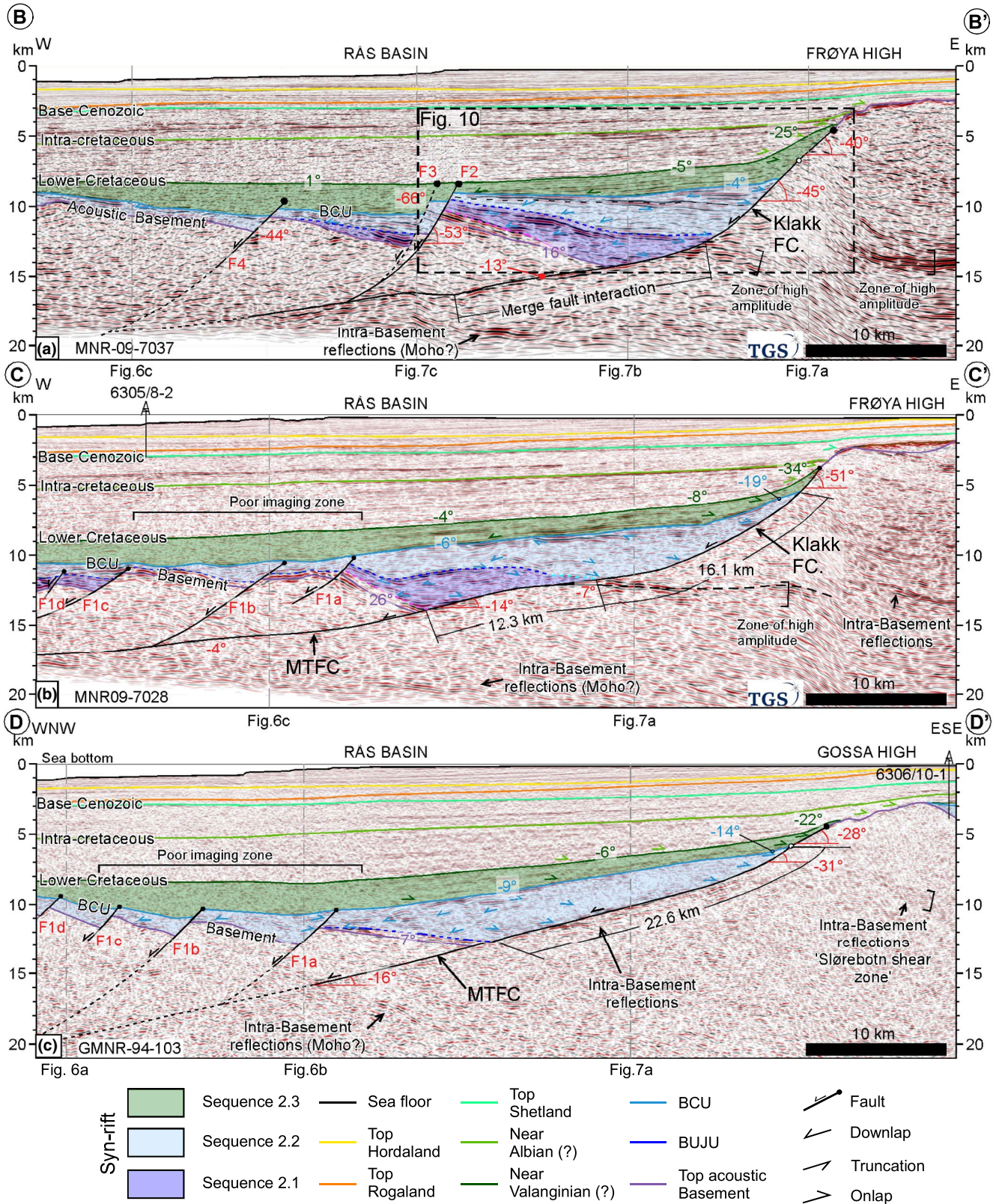


FIGURE 6 Depth converted dip cross-sections showing the variation along strike of the supradetachment basin. Location Figure 4

heave decrease northward from ca. 17 to 6 km (Figures 4–7; and Table 1). All segments show a listric geometry in cross-section. The fault segments decrease in dip with

depth from ca. $54^\circ \pm 9^\circ$, to $12^\circ \pm 4^\circ$ where they merge onto an intra-basement band of high-amplitude reflections at 13.8 to 14.7 km depth (Figures 5–7, and Table 1).

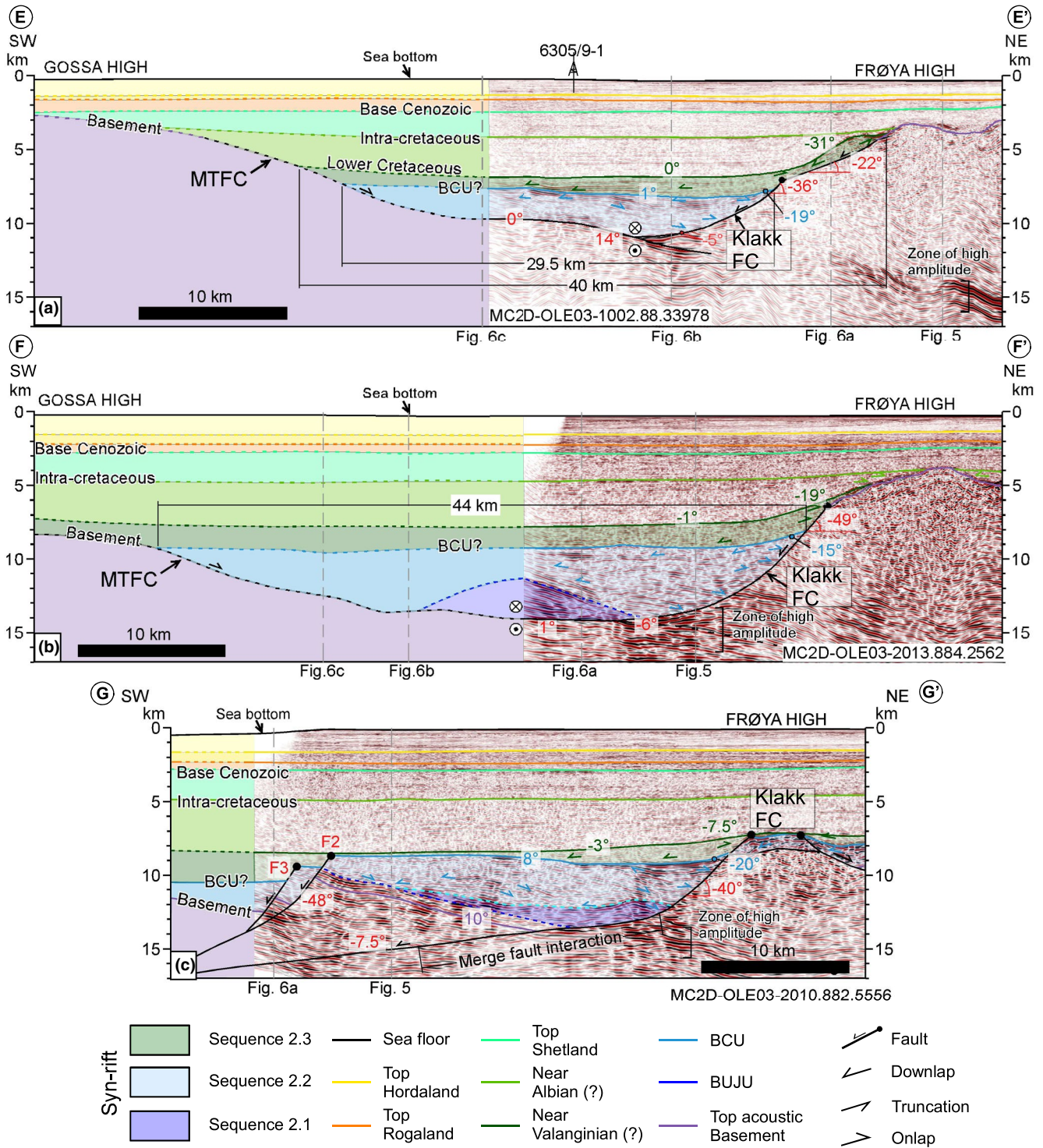


FIGURE 7 Depth converted strike cross-sections showing the variation along dip of the supradetachment basin. Location Figure 4

Three major faults segments compose the MTFC in this area, creating a zig-zag plan-view geometry (Figure 4). Heaves increase northwards from ca. 3 to 33 km (Figures 6 and 7 and Table 1). The southern fault segment shows a NE-SW-striking with a down-to-the-northwest low-angle planar geometry that delineates the northwestern part of the Gossa High, and features heaves up to ca.

12 km (Figures 4 and 6c and figure 8b in Osmundsen & Péron-Pinvidic, 2018). The central fault segment displays a WNW-ESE-striking and a listric geometry in plan-view with heaves of ca. 12 to 30 km (Figure 4). The northern fault segment shows a WNW-ESE-striking with a down-to-the-northwest listric geometry in cross-section, where the upper part dips ca. 31°, shallowing to ca.

TABLE 1 Characterisation of the Klakk FC and MTFC in the cross-section in the dip direction. Location Figure 2

Main fault strand			Upper dip	Lower dip	Displacement	Heave	Throw
Section	Figure	Geometry	Grade	Grade	(m)	(m)	(m)
A-A'	5	Listric	49	6	21,013	17,944	9809
B-B'	7a	Listric	45	9.5	23,207	19,293	11,565
C-C	7b	Listric	51	4	33,427	30,697	11,475
D-D'	7c	Listric	31	16	28,075	26,200	8885

13 km depth (Figures 4, 6 and 7 and Table 1). Figures 6b and 7 show the interaction of the Klakk FC and MTFC in cross-section. In seismic profile 6b, the Klakk FC has an upper part dipping westward at ca. 51°, shallowing to ca. 7° at ca. 14 km when it joins the strand of the MTFC, whereas the MTFC has an upper part dipping ca. 14°, shallowing to 4° at ca. 15.3 km depth. This section shows the highest displacement in the study area of ca. 33 km (Table 1).

A band of high-amplitude intra-basement seismic reflections underlies the supradetachment basin (Figures 4–7). This band is the seaward continuation of proposed Palaeozoic shear zones identified into the Frøya and Gossa Highs (Figures 5 and 7; Muñoz-Barrera et al., 2020; Osmundsen & Péron-Pinvidic, 2018). The Klakk FC and the MTFC merge onto this intra-basement band where the fault segments dip less than ca. 14° (Figures 5 and 7). In cross-section, the intra-basement band is ca. 16 to 18 km long and ca. 0.7 to 1.3 km thick at the Klakk FC, whereas is ca. 32 km long and 1.2 km thick at the MTFC (Figures 5–7). Muñoz-Barrera et al. (2020) identify a good match between the geometry of the shear zone and the gravity anomaly map on the Frøya High. In the location of the supradetachment basin studied here, the gravity anomaly map shows a semi-elliptic geometry with values of 10–30 mGal between the Frøya and Gossa Highs (Figure 4b). This semi-elliptic geometry matches very well with the geometry and location of the supradetachment basin.

4.2 | Intra-basinal faults

Down-to-the-W/SW intra-basinal normal faults striking N-S and NNE-SSW dissect the supradetachment basin towards the northwest (Figures 4–7). These intra-basinal faults dissect the basinal deposits as well as the acoustic basement and show planar to listric geometries in cross-section that dip ca. 47° ± 13°, and with heaves in the range of 0.1–2 km (Figures 4–7 and Table 2). The cumulative heave of these intra-basinal faults decreases northward (Figure 4e). Some of these intra-basinal faults merge with

the Jan Mayen Lineament towards the northeast, which forms an imbricate fan geometry in plan-view (Figure 4). Neither the seismic profiles nor the gravity anomaly map shows a continuation of the NE-SW Jan Mayen Lineament into the supradetachment basin (Figures 4a,b and 7).

5 | SEISMIC STRATIGRAPHY OF THE SUPRADETACHMENT BASIN

We divided the sedimentary fill into three seismic megasequences within the supradetachment basin. Seismic megasequence 1 has only one sequence in the study area; seismic sequences 2.1, 2.2 and 2.3 form seismic megasequence 2; whereas seismic sequences 3.1, 3.2 and 3.3 comprise seismic megasequence 3 (Figures 3 and 5). For seismic megasequence 3, however, we describe here only the immediately overlying succession (sequence 3.1), since a detailed description of this overall seismic megasequence succession falls beyond the scope of this study. We recognise eight seismic facies: sheet, wedge, trough, “U” channel, channel fill, fan, mound and basin fill, which we named based on their external form (Figure 8; *sensu* Sangree & Widmier, 1979). The lack of borehole control below 4.5 km at the Rås basin does not allow us to define the exact depositional elements and corresponding depositional system. In addition, the age of each seismic sequence and seismic megasequences described is unknown.

5.1 | Seismic megasequence 1

Seismic megasequence 1 is composed by one seismic sequence (SS-1.1) that is bounded below by reflections in concordant contact with the acoustic basement (Figures 9a and 10b), and above by truncations or reflections in concordant contact with sequence 2.1 (Figures 9a,b, 10a, and 11). Seismic sequence 1.1 shows a tectonic contact with the Klakk FC and the subsidiaries faults associated with the Jan Mayen Lineament (Figures 5–7). The intra-basinal faults do not show evidence of thickness changes into the footwalls and hanging walls.

TABLE 2 Characterisation of the intra-basinal faults in the cross-section in the dip direction. Location Figure 2

Fault strands on Rås Basin						
Section	Fault	Geometry	Dip	Displacement	Heave	Throw
			Degrees	(m)	(m)	(m)
A-A'	F1a	Planar@Basement	62	155	88	145
A-A'	F1b	Planar@Basement	66	555	240	522
A-A'	F1c	Planar@Basement	54	492	302	415
A-A'	F2	Planar@Basement	37	4892	3913	2966
A-A'	F2	planar@BCU	37	1984	1581	1191
A-A'	F2a	Planar@Basement	54	855	497	693
B-B'	F2	Planar@Basement	53	2329	2152	960
B-B'	F3	Planar@Basement	66	3214	2927	1378
B-B'	F4	Planar@Basement	44	6115	5389	2942
B-B'	F2	Planar@BCU	53	2115	1874	1099
C-C	F1a	Planar@Basement	27.8	2923	1863	2232
C-C	F1b	Planar@BCU (a)	27.8	912	505	715
C-C	F1c	Planar@BCU (b)	27.8	870	522	803
C-C	F1d	Planar@Basement	30	2199	1932	1081
C-C	F1c	Planar@BCU	30	1327	1184	575
D-D'	F1a	Planar@Basement	48.4	1416	903	1089
D-D'	F1a	Planar@BCU	48.4	449	315	364
D-D'	F1b	Planar@Basement	48.5	1329	879	1028
D-D'	F1b	Planar@BCU	48.5	448	331	282
D-D'	F1c	Planar@Basement	48.6	1063	680	846
D-D'	F1d	Planar@Basement	43	714	497	514

This seismic sequence displays a sheet-like external form and is east dipping (16° – 30°) with an average true stratigraphic thickness of ca. 0.6 km and a maximum thickness up to ca. 1.3 km. Seismic sequence 1.1 is dominated by sheet seismic facies, which is composed by high-amplitude, continuous reflections (Figures 8, 9a,b, and 10a,b).

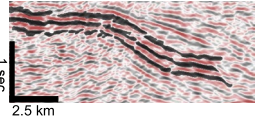
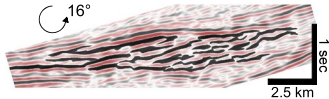
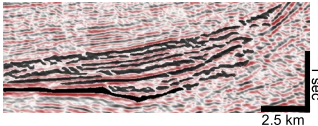
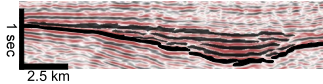
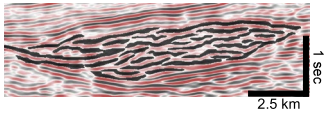
5.2 | Seismic megasequence 2

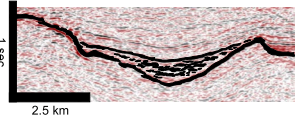
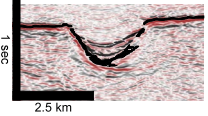
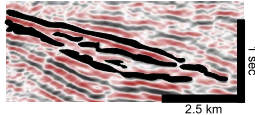
Megasequence 2 represents the syn-tectonic deposits within the supradetachment basin. We define three seismic sequences based on the presence of high-amplitude, continuous reflections, thickness changes into footwall and hanging wall, and seismic reflection terminations.

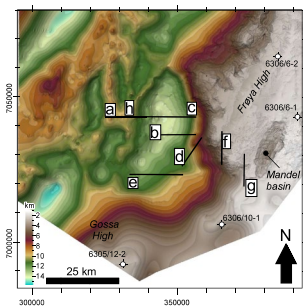
5.2.1 | Seismic sequence 2.1 (SS-2.1)

The base of seismic sequence 2.1 is marked by downlapping seismic reflection terminations, particularly in the

immediate hanging wall of the Klakk FC, or reflections in concordant contact with SS-1. Whereas the top of seismic sequence 2.1 is marked by a continuous high-amplitude trough seismic reflection (Figures 9 and 10). Seismic sequence 2.1 shows a tectonic contact with the Klakk FC, MTFC and intra-basinal faults, and has a wedge-shaped geometry that thickens towards these faults (Figures 9, 10 and 12). This seismic sequence typically has true stratigraphic thickness of up to 6 km, but locally up to ca. 12 km where the Klakk FC join the MTFC (Figures 5 through 7). Seismic sequence 2.1 shows a post-depositional eastward dip up to 30° (Figures 5, 7, 9, and 10). It is composed by wedges with cliniform and mound seismic facies in the immediate hanging wall of the Klakk FC and MTFC, and fan seismic facies in the immediate footwall of the intra-basinal faults (Figures 8–12a). The interpretation of downlaps and toplaps within the wedge allow us to divide it into five packages comprising sigmoidal internal reflections which we interpret as a package of cliniforms overlain by a single fan package (Figures 10 and 11). These cliniforms have thickness of ca. 0.308 s TWT (847 m) to ca. 0.342 s TWT (940 m), and their foreset angles vary between ca. 25° and 35° . Consequently, we used the topset

Seismic Facies	Contact	Reflections characteristics	Reflections	Interpretation
Sheets	Base: Concordant Top: Concordant or truncation	Internal configuration: Parallel Continuity: Continuous Amplitude: High Frequency: Moderate		Shallow marine clastic deposits in a shelf depositional system
Wedge	Base: Downlap Top: Onlap	Internal configuration: sigmoid-to-the-west (when we flat the base 16° anticlockwise) Continuity: Moderate Amplitude: High to moderate Frequency: Broad to moderate		Clinoforms generated by prograding sediments in a shelf environment (sensu Patruno & Helland-Hansen 2018)
Fan	Base: Downlap Top: Onlap	Internal configuration: Parallel Continuity: Continuous Amplitude: Moderate Frequency: High		Fan complex deposited in the basin slope and basin floor
Basin fill	Base: Downlap Top: Concordant	Internal configuration: Parallel Continuity: Continuous Amplitude: Moderate Frequency: Moderate		Onlapping filling in a basin floor depositional system. This facies was deposited in a relatively low-velocity turbidity current environment.
Mound	Base: Downlap or concordant Top: Onlap or toplap	Internal configuration: Chaotic Continuity: Discontinuous Amplitude: Moderate Frequency: Moderate		Elongate mounds deposited by relative high-velocity turbidity currents in deep-water environments.

Seismic Facies	Contact	Reflections characteristics	Reflections	Interpretation
Trough	Base: Onlap Top: Concordant	Internal configuration: Chaotic Continuity: Discontinuous Amplitude: Moderate Frequency: Broad		Fill of slope channel system in basin slope depositional system
"U" channel	Base: Onlap Top: Concordant	Internal configuration: Parallel Continuity: Continuous Amplitude: High Frequency: Low		Canyons at the top of fault scarp
Channel fill	Base: Bidirectional onlap Top: Concordant	Internal configuration: Parallel Continuity: Continuous Amplitude: High Frequency: Low		Channel fills in a continental depositional system



Location of seismic profiles described in the seismic facies:

- a: Sheets
- b: Wedge
- c: Fan
- d: Basin Fill
- e: Mound
- f: Trough
- g: "U" Channel
- h: Channel fill

Widmier (1979).

FIGURE 8 Seismic facies identified within the study area. Seismic facies description and interpretation based on Sangree and Widmier (1979)

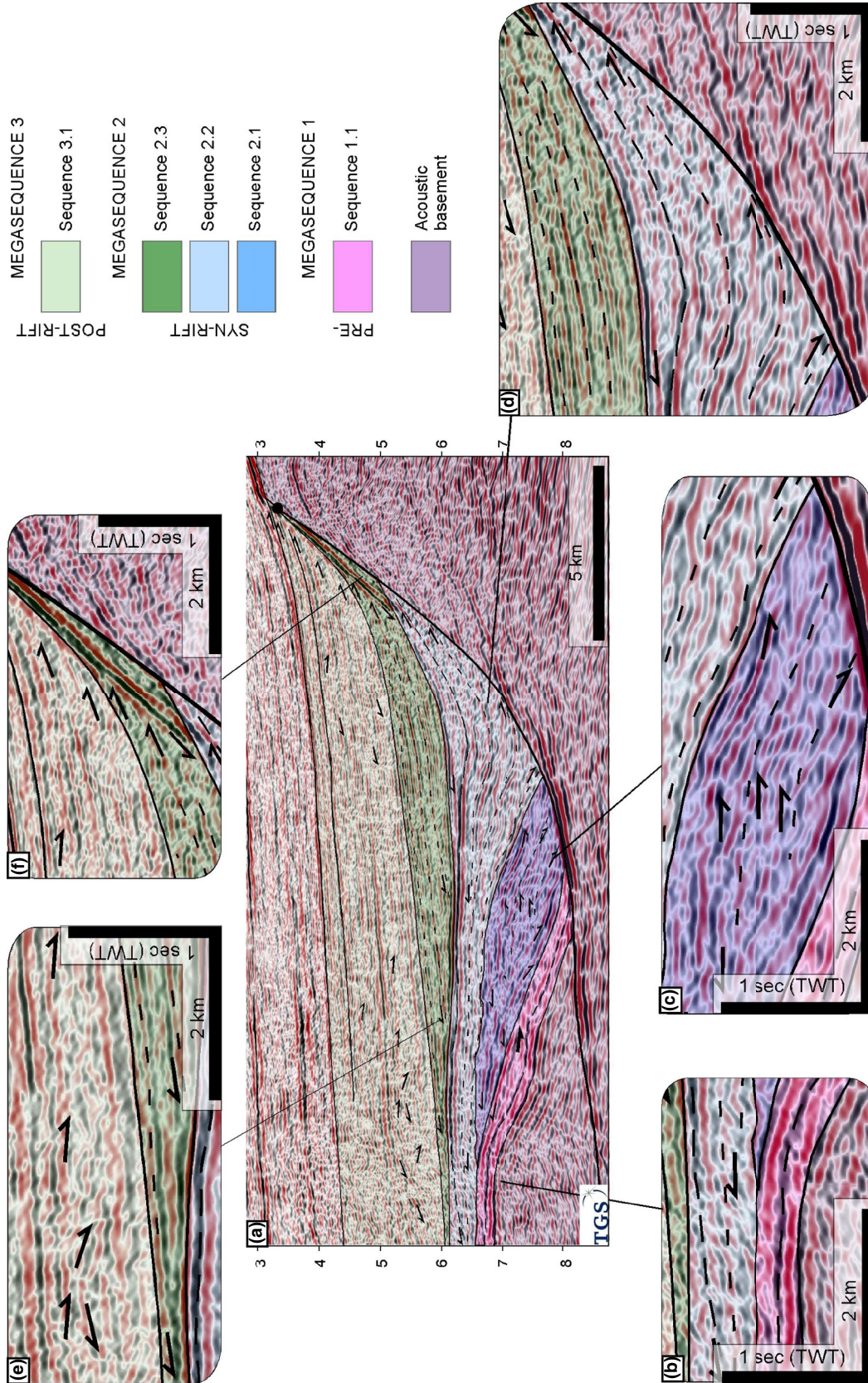


FIGURE 9 Pre-, Syn- and post-rift deposits identified within the supradetachment basin. (a) zoom of Figure 5 in the immediate footwall of the Klakk FC. (b) Zoom of parallel continuous reflections within seismic sequence 2.1 showing some toplaps and onlaps terminations. (c) Zoom of onlap seismic terminations of seismic sequence 2.2 on the Klakk FC. (d) Zoom of downlap seismic terminations of seismic sequences 2.3. (e) Zoom of onlap seismic terminations of seismic sequences 2.3 on the Klakk FC

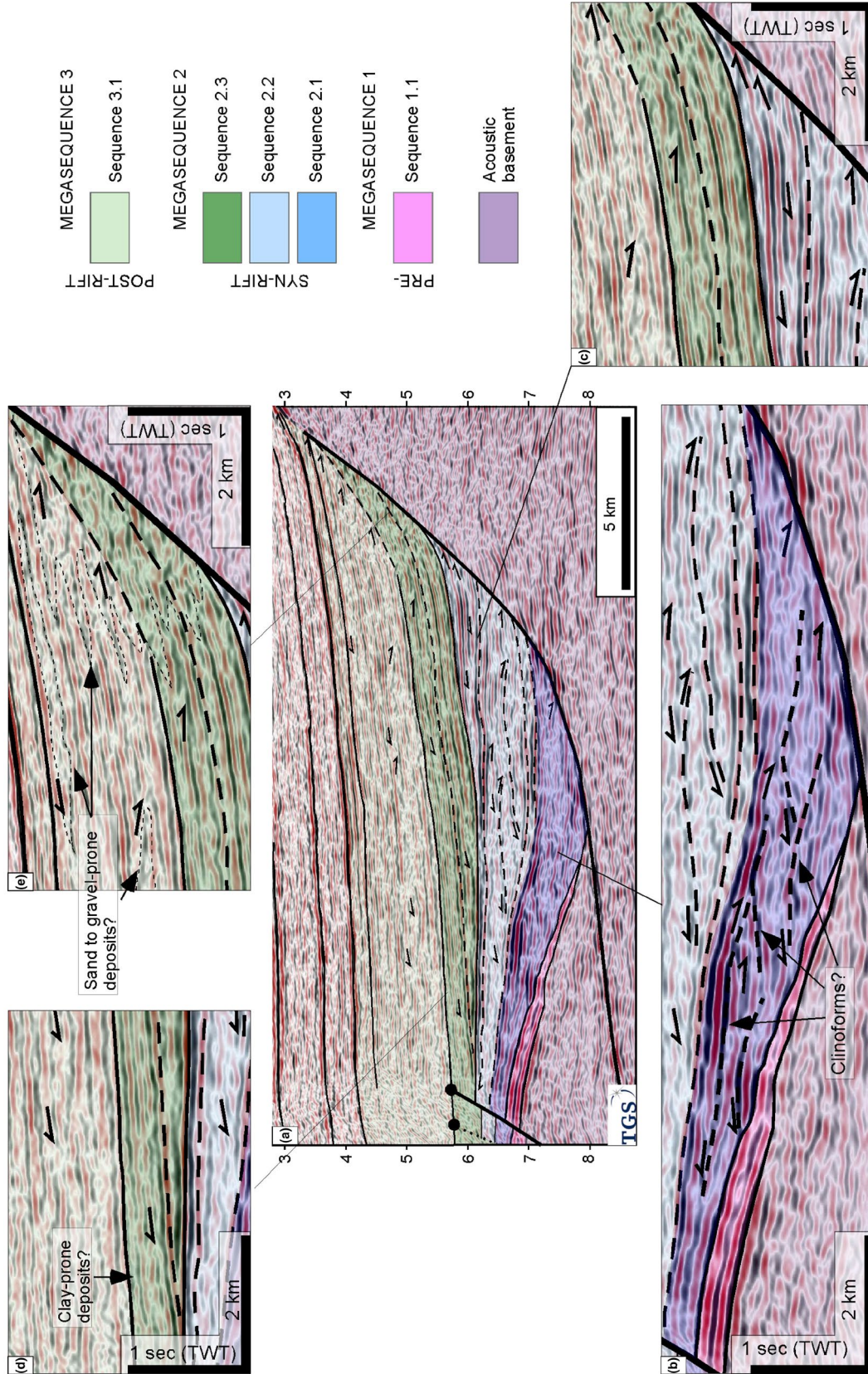


FIGURE 10 Pre-, Syn- and post-rift deposits identified within the supradetachment basin. (a) Zoom of Figure 7a in the immediate footwall of the Klakk FC. (b) Zoom of sequence 2.1 showing downlap and toplap seismic termination. (c) Zoom onlap seismic terminations of sequence 2.2 on the Klakk FC. (d) Zoom of downlap seismic terminations of sequence 2.3. (e) Zoom of onlap seismic terminations on the Klakk FC

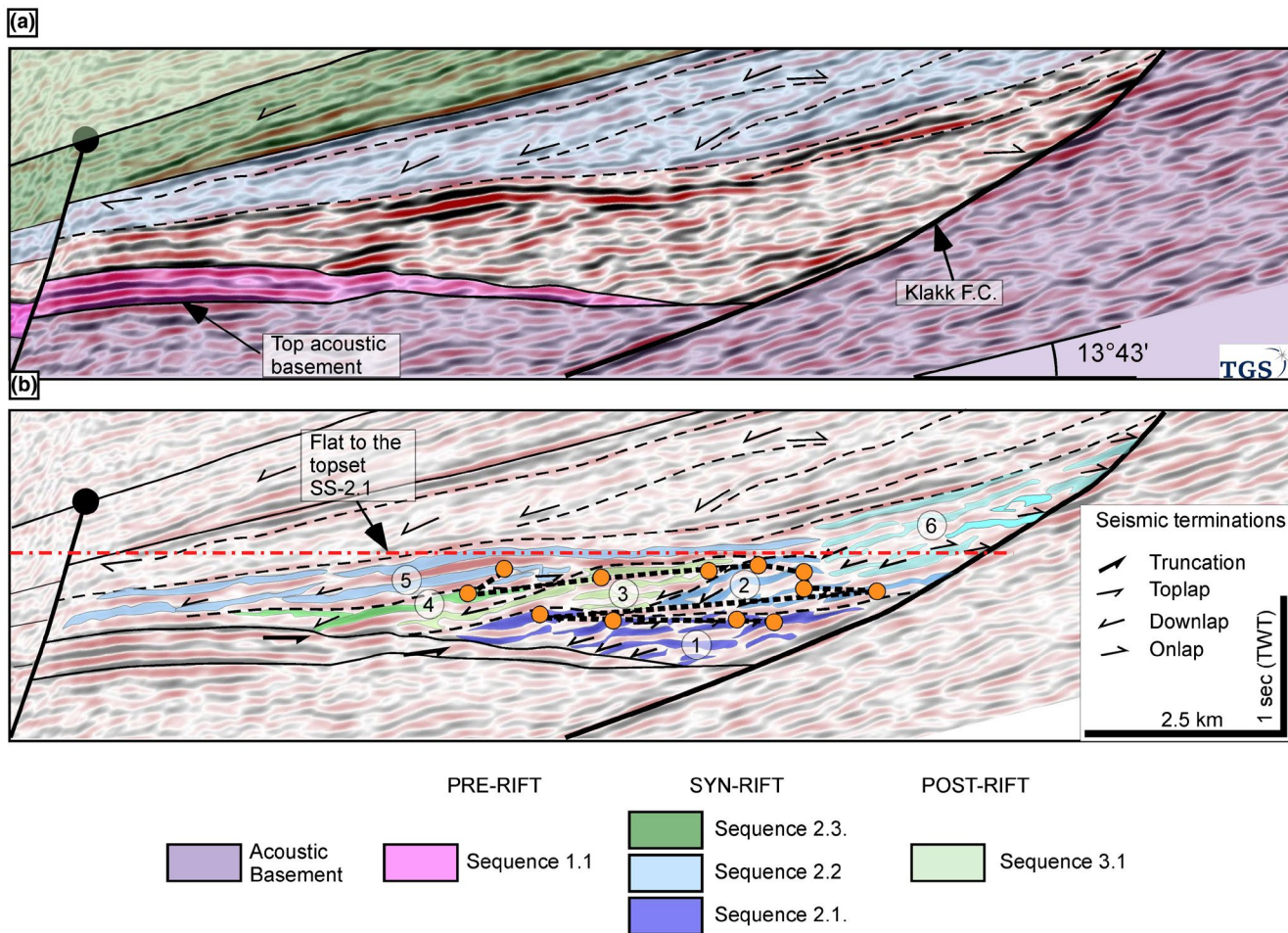


FIGURE 11 Rotation of Figure 10b using as datum the topset of sequences 2.1. (a) Seismic sequence 2.1 uninterpreted. (b) Interpretation of five clinoform packages and one fan package into the seismic sequence 2.1. The numbers refer to clinoform packages number 1 through 5, and a trapezoidal fan package, 6, which are discussed in the text

of the upper clinoform interpreted in Figure 10 as a pin to rotate the seismic profile (Figure 11). The wedge with sigmoidal internal configuration required a rotation of ca. 14° seawards in order to restore the upper clinoforms topset to horizontal (Figure 11).

5.2.2 | Seismic sequence 2.2 (SS-2.2)

Seismic sequence 2.2 is bounded below by downlapping seismic terminations on the top of SS-2.1, above by a continuous high-amplitude trough reflection and shows a tectonic contact with the Klakk FC, MTFC and subsidiary faults (Figures 5–7, 9, and 10). This seismic sequence shows a wedge external geometry thickening towards the Klakk FC and MTFC (Figures 5, 7, 9, 10, and 12). The true stratigraphic thickness of SS-2.2 decreases towards the north (ca. 10 km; Figures 5–7) and has a maximum true stratigraphic thickness of ca. 23 km towards the MTFC (Figure 6c) and a maximum true vertical thickness of ca. 3 km towards the location

of cross-section A-A' (Figures 5 and 12c). Seismic sequence 2.2 is composed mainly of fan seismic facies in the immediate footwall of the Klakk FC, with sporadic presence of mound, sheet and channel seismic facies towards the west (Figures 8–10). The top of this seismic sequence forms a smooth surface dipping 8° west that covers the entire spoon-shaped basin and is dissected towards the west by intra-basinal faults in plan-view (Figure 11a). Seismic sequence 2.2 displays a post-depositional landward rotation immediately above the Klakk FC from ca. 22° to the west to ca. 26° to the east (Figures 5–7). The structural restoration shows a reduction of ca. 7° in dip angles because of thermal subsidence and compaction (Figure 5). The seismic resolution varies between the different seismic vintages, where we could separate seismic sequence 2.1 from 2.2 only in the majority of seismic MNR. Consequently, we created an isopach map between the basement and the top of the Spekk Formation, which allow defying the total accommodation within the supradetachment basin (seismic sequence 2.1 and 2.2 combined). This map shows

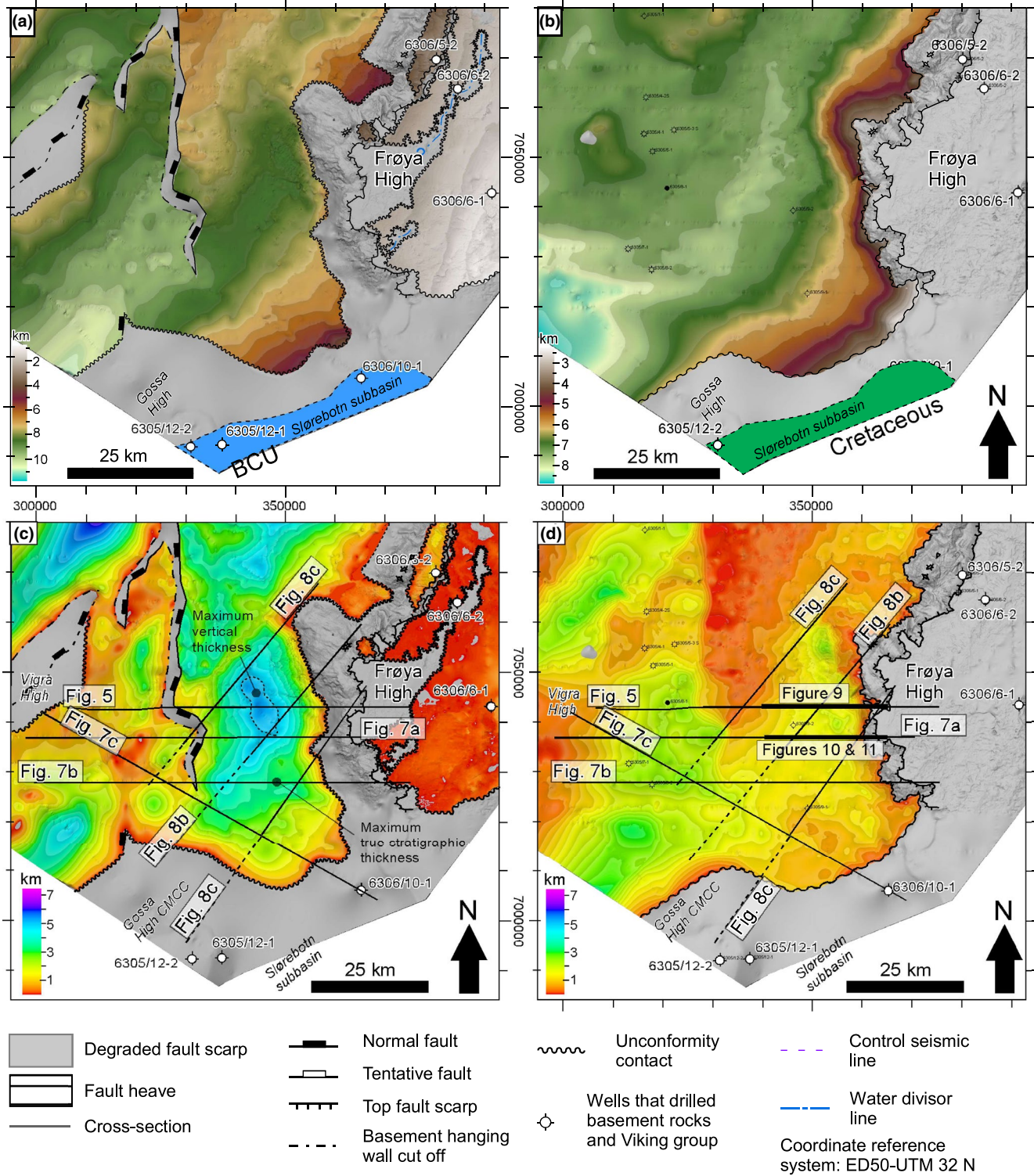


FIGURE 12 Structural maps and isochore maps of Megaseismic sequence 2 (a) Structural map at the top of seismic sequence 2.2 (BCU), (b) Structural map at the top of seismic sequence 2.3 (near top Valenginian), (c) Isochore map between basement (Figure 4a) and top of seismic sequence 2.2 (Figure 12a), (d) Isochore map between top seismic sequence 2.2 (Figure 12a) and top of seismic sequence 2.3 (Figure 12b)

an average true vertical thickness (*sensu* Groshong Jr, 2006) of ca. 4 km with a maximum true vertical thickness (*sensu* Groshong Jr, 2006) of ca. 6 km towards the northern part of the basin (Figures 5 and 12c).

5.2.3 | Seismic sequence 2.3 (SS-2.3)

The base of seismic sequence 2.3 is limited by the down-lap onto SS-2.2, at the top by the first reflection that

covers the entire supradetachment basin and is in tectonic contact with the faults sets one and two (Figures 5–7 and 9–11). This seismic sequence shows a sheet drape external form with fan external forms towards the Klakk FC and MTFC (Figures 5–9). The true stratigraphic thickness increases towards the north, changing from ca. 3 km around the Gossa High to ca. 7 km towards Frøya High (Figures 5–7 and 9–12d). The true vertical thickness is up to ca. 3 km, where the maximum vertical thickness is located in the immediate hanging walls of the intra-basinal faults (Figure 12d). Seismic sequence 2.2 is composed of (i) fan seismic facies located towards the Klakk FC, MTFC and intra-basinal faults; (ii) sheet seismic facies towards the footwall of the intra-basinal faults; and (iii) channel seismic facies on the eroded fault scarp (Figures 8–10).

5.3 | Seismic megasequence 3

Megasequence 3 represents the post-rift deposits within the supradetachment basin. These deposits draped the syn-rift deposits and do not exhibit any fault displacement. Three seismic sequences comprise Megasequence three (Figures 3 and 5). Seismic sequences 3.2 and 3.3 have borehole control, whereas 3.1 does not.

5.3.1 | Seismic sequence 3.1 (SS-3.1)

Seismic sequence 3.1 covers the tips of the intra-basinal faults and is not offset by any fault (Figures 5–7). This seismic sequence is limited at its base by downlapping and concordant seismic reflection terminations over the top of SS-2.3, whereas the top of the seismic sequence is marked by a high-amplitude continuous peak (black; Figures 5–7). In addition, it shows onlapping reflection terminations onto the Klakk FC and MTFC scarps. Seismic sequence 3.1 has an overall tabular geometry that thins towards the Klakk FC and MTFC, with a maximum vertical thickness of ca. 4 km towards the west. Consequently, this seismic sequence shows onlap seismic terminations on the fault scarps and the top of seismic sequence 2.3 (Figures 5–7, 9, and 10). Sheet seismic facies dominates this sequence and shows high-frequency, semi-continuous reflections that dip gently towards the west. Fan seismic facies are located in the vicinity of the Klakk FC fault scarp, while mound seismic facies can be observed up to 20 km from the Klakk FC (Figures 8 and 9e,f). Seismic image quality decreases towards the west, where reflections tend to have a wavy to hummocky internal configuration.

6 | DISCUSSION

6.1 | Regional evolution of the Møre–Vøring rifted margin segments

We postulate a model for the evolution of the supradetachment basin based on integrated seismic stratigraphy and structural observations (Figure 13). No wells have been drilled in this area; therefore, any specific age estimates discussed are highly tentative, and based on extrapolations of ages reported in the wells within the Slørebotn Subbasin, the southern Halten Terrace and the Frøya High (Figure 2), and supported with information from other published studies (i.e., Elliott et al., 2015; Jones et al., 2020; Jongepier et al., 1996; Ravnås et al., 2014).

6.1.1 | Pre-thinning

Seismic megasequence 1 represents the lowest level of stratigraphy within the basin and is characterised by the absence of stratigraphic evidence (across-fault stratigraphic thickness contrast) for syn-kinematic “growth” (Figures 7 and 13a). We therefore interpret that Megasequence 1 represents the pre-thinning stage. Pre-thinning deposits in this context may correspond to pre-rift deposits (Upper Devonian–Middle Permian) or quiescent periods between major rift phases (Middle Triassic–Lower Jurassic and Lower Cretaceous–Late Cretaceous) based on the models for the evolution of the Norwegian Margin (Blystard et al., 1995; Faleide et al., 2008; Peron-Pinvidic et al., 2013; Peron-Pinvidic & Osmundsen, 2018; Tsikalas et al., 2012). Seismic megasequence 1 overlies the acoustic basement and displays parallel reflections dipping up to 37° towards the east (Figure 6); Upper Triassic deposits within the Slørebotn Subbasin to the southeast show sheet-like seismic facies dipping up to 50° (figure 2 in Jongepier et al., 1996; figure 8b in Osmundsen & Péron-Pinvidic, 2018; and figure 1.2 in Bukta, 2018). Müller et al. (2005) demonstrate a lack of tectonic activity in the region during the Carnian (evaporites deposits) to Rhetian (Grey Beds) in the Norwegian margin during this time. Well penetrations on the Frøya High, within the Froan Basin and on the Halten Terrace (e.g., wells 6306/6-1, 6305/12-1, 6307/1-1S and well 6406/11-1S), confirm the presence of Lower to Middle Triassic deposits in the footwall of the Klakk FC. Based on all of the above, we therefore speculate an age of Middle Triassic to Early Jurassic for seismic megasequence 1 (Figures S1–S3).

6.1.2 | Early-rift architecture and deposits

At the base of seismic megasequence 2, seismic sequence 2.1 shows fault-ward expanding wedge-shaped

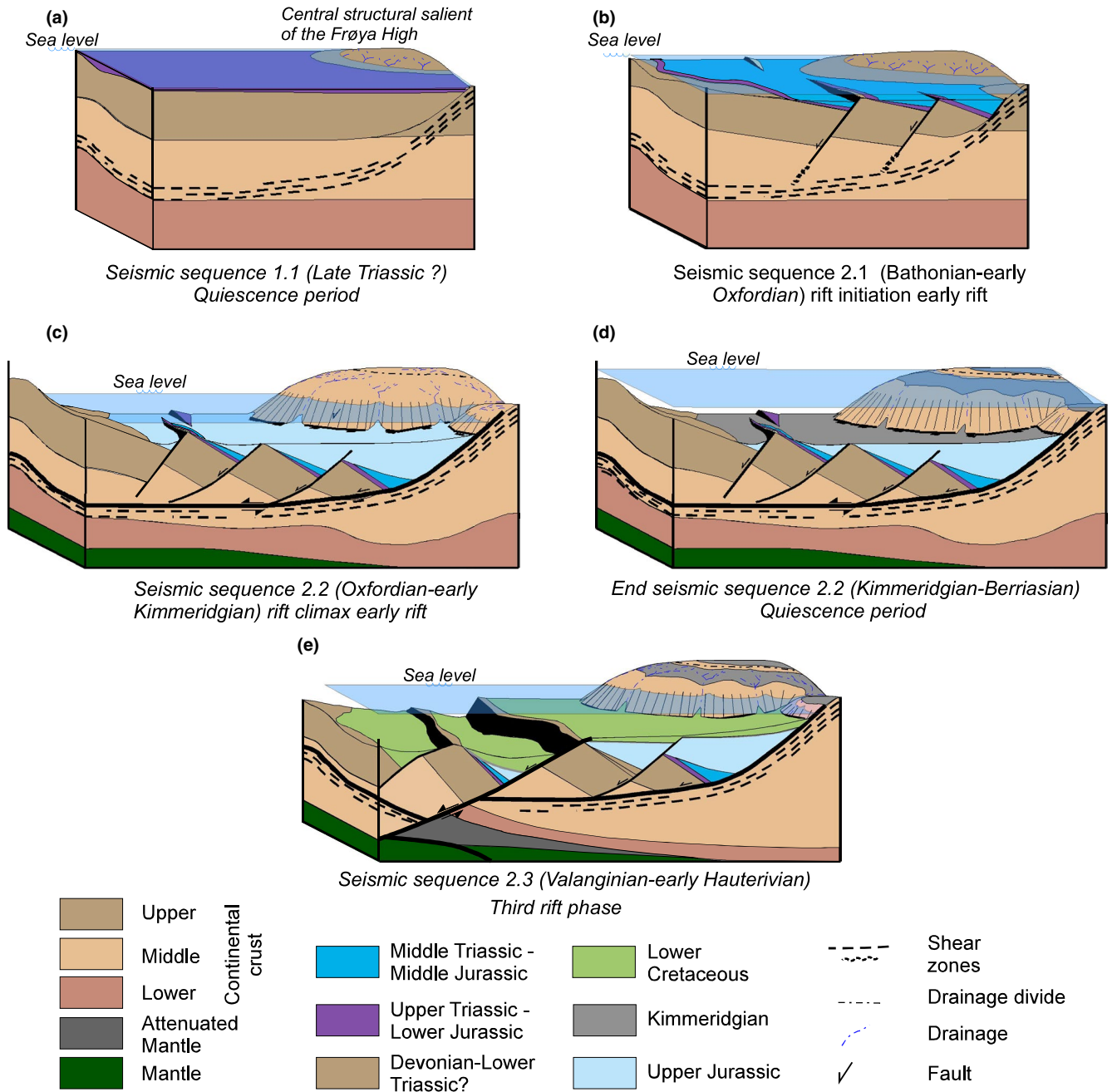


FIGURE 13 Schematic evolution model for the evolution of the spoon-shaped supradetachment basin in the necking domain of the Norwegian rifted margin. (a) Seismic sequence 1.1, Pre-rift, which may represent a quiescence period during the late Triassic. (b) Seismic sequence 2.1 associated to a mild rifting during the middle Jurassic. (c) Seismic sequence 2.2, rift climax in the Late Jurassic representing the second rift phase (Thinning). (d) End of seismic sequence 2.2 (BCU), which may represent a quiescence period. (e) Sequence 2.3 representing the third rift phase (Hyperextension). Deformation migrates basin-wards and creates the coupling point

geometries overlying the seismic megasequence 1 in the immediate hanging walls of the Klakk FC and the intrabasin faults (Figures 5–7, 11 and 13b). Figures 10 and 11 show a series of bundles of sigmoidal reflections, which we interpret as a total of six seismic-stratigraphic packages: five distinct clinoforms packages and one fan-shaped package. The clinoform packages are ca. 2–4 km wide in dip-section from the eastward part of the topset,

to the westward part of the bottom set, with foresets between ca. 25° and 35° and ca. 900 m high (Figure 11). These large foresets heights may indicate substantial water-depth in the hanging wall of the Klakk FC at this time, and they are of similar dimensions to Gilbert-type deltas in the Corinth rift; with a radius of up to 4 km, these have foresets up to 800 m high in the Kerinitis delta (Gawthorpe et al., 1994; Rohais et al., 2007) and

the Vouraikos delta (Ford et al., 2013). *Clinoform package one* shows a continuous basinward downlapping, and basinward movements of the topset break point trajectory that we interpret as a phase of clinoform progradation (Figure 11). The overlying *package two* marks a landward shift in the topset break point indicating a retrogradation of the clinoforms due to an increase in accommodation space. *Packages three and four* display a return to basinward-stepping downlaps onto the underlying packages one and two, and, in the western part of the basin fill, onto Megasequence 1, marking a second phase of progradation during forced regression. *Package five* shows landward-stepping onlap onto packages 3 and 4, reflecting a stage of clinoform retrogradation due to an increase in accommodation space or reduced sediment supply. *Package 6* does not show a similar sigmoidal geometry to packages 1–5. Instead, package 6 shows a trapezoidal fan geometry downlapping onto packages two and five and onlapping the Klakk FC. We interpret the change to a fan morphology in package six to reflect a substantial increase in accommodation with respect to sediment supply, associated with an increase in fault displacement and initiation of starved-fill conditions (*sensu* Chiarella et al., 2020; Pechlivanidou et al., 2018). We interpret that the clinoforms and overlying fan deposits are syn-tectonic strata associated with onset activity of the Klakk FC based on: (i) the wedge-like overall form of seismic sequence 2.1, thickening towards the Klakk FC and (ii) the proposed overall increase in accommodation in the hanging wall of the Klakk FC.

Syn-rift deposits of Mid-Late Jurassic age have been recognised in the Norwegian margin (e.g., Blystad et al., 1995). At the Slørebotn Subbasin, Jongepier et al. (1996) propose that early-rifting started in the Bathonian based on the occurrence of subaerial to subaqueous alluvial fans and evidence of resedimentation, syn-sedimentary deformation and rapid facies changes around structures. At the Halten Terrace, two hypotheses have been proposed for the onset of Jurassic rifting, early-middle Callovian (Elliot et al., 2015) and late Callovian-early Oxfordian (Jones et al., 2020). Elliot et al. (2015) propose that early rifting started in the northern part of the Frøya High, along the Vingleia FC, based on changes in thickness and facies of coastal plain to shallow marine sediments around the Vingleia Fault. Jones et al. (2020) propose that early-rift started later during the late Callovian-early Oxfordian based on biostratigraphy from the Fenja Oil Field. In addition, Jones et al. (2020) note that the earliest rift deposits in the hanging wall in the Vingleia FC were likely sources from the Sklinna Ridge rather than the Frøya High. Ultimately this forms a broader age range for activity of faults bounding the Frøya High, with early rift stratigraphy deposited from the Bathonian in the south at the Slørebotn Subbasin,

to early Oxfordian in the north around the Vingleia FC. Based on all of the above, we therefore speculate that the onset of rifting recorded in Megasequence 2 within the supradetachment basin occurred in Bathonian to early Oxfordian times, which corresponds to the rift-initiation (*sensu* Prosser, 1993) of the thinning deformation phase.

6.1.3 | Late-rift architecture of a major fault complex

Seismic sequence 2.2 records a thick, wedge-shaped sedimentary package up to ca. 23 km true stratigraphic thickness, which is in tectonic contact with the Klakk FC and MTFC, and with post-depositional landward rotation of up to 40° (Figures 5–7, 9 and 13c). The thickness of the sedimentary package, the landward post-depositional rotation, and the depositional and tectonic contacts of seismic sequence 2.2 lead us to interpret them as deposits related to supradetachment basin formation, i.e., deposited during the main stage of detachment faulting, similar to other spoon-shaped supradetachment basins in Norway, such as the Hornelen, Kvamshesten and Solund basins (see section 6.2; Osmundsen et al., 1998; Seranne & Seguret, 1987; Vetti & Fossen, 2012). We therefore interpret seismic sequence 2.2 as recording the continuation of rift activity with accumulation of substantial displacements along the Klakk FC and MTFC, which by this stage had developed into low-angle detachment-style faults.

A major rift event has been reported within the Slørebotn and southern Halten Terrace during the Callovian to Middle Tithonian times (Elliot et al., 2015; Jones et al., 2020; Jongepier et al., 1996). Wells in these areas show alluvial fans to slumps, turbidites and fine-grained pelagic deposits (Jones et al., 2020; Jongepier et al., 1996). In addition, figure 8 in Jongepier et al. (1996) and figure 15 in Jones et al. (2020) show that these deposits have a post-depositional landward rotation up to 50°. Jongepier et al. (1996) reported a transition from continent- to marine-dominated conditions from Callovian to early Kimmeridgian in the Slørebotn, and a major fault block rotation during the early to middle Volgian. Jones et al. (2020) recognise a “peak-rift” during the middle-late Oxfordian based on biostratigraphical data in shale beds that separate coarse-grained deposits in the Fenja Oil Field. Elliot et al. (2015) recognise an onset activity of the Vingleia FC during the Oxfordian that led to the fault scarp erosion with possible deposition of fan deltas, confirmed through later investigation in Jones et al. (2020), which highlight the exhumation and uplift of the Frøya High during the Oxfordian to Kimmeridgian. Several authors have shown that the second rifting phase (thinning *sensu* Peron-Pinvidic et al., 2013) on the Norwegian margin caused the

generation of high-displacement faults such as the Klakk FC, Ytreholmen Fault Zone and the outer strand of the MTFC (Blystad et al., 1995; Faleide et al., 2008; Peron-Pinvidic et al., 2013; Tsikalas et al., 2012). The thinning phase is characterised by strain localisation and thinning of the continental crust from ca. 30 to 10 km (Naliboff et al., 2017; Osmundsen & Péron-Pinvidic, 2018; Peron-Pinvidic et al., 2013). We interpret therefore that seismic sequence 2.2 represents this deformation stage, where the Klakk FC and the outer strand of the MTFC generated the necking domain of the Norwegian rifted margin and caused the spoon-shaped supradetachment basin. This deformation may represent the rift climax (*sensu* Prosser, 1993) of the thinning deformation phase.

6.1.4 | Inter-rift period

The upper boundary of seismic sequence 2.2 is represented by a continuous high-amplitude trough reflection within the basin and a tectonic contact located on the fault scarps of the Klakk FC, the outer strand of the MTFC and the intra-basinal faults (Figures 4–6 and 13d). A similar seismic character has been identified in the Halten Terrace, where it corresponds to the top of the Spekk Formation in different wells, for example, wells 6406/12-1S and 6406/12-3B (Bell, Jackson, Elliott, et al., 2014; Elliott et al., 2015; Jones et al., 2020; Norwegian Petroleum Directorate, Factpages, 2000; Wilson et al., 2015). This criterion has been used by some authors to interpret the BCU in the Rås Basin (e.g., Gernigon et al., 2020; Osmundsen et al., 2016). Therefore, we use the same criteria to identify the BCU within the study area.

The Spekk Formation is proposed to have covered the Gossa High and almost covered the whole Frøya High constrained by based on well data and seismic interpretation (Chiarella et al., 2020; Jongenpier et al., 1996). On the Frøya High, the biostratigraphy, geochemistry and lithological data of wells 6306/6-1 and 6407/10-3 show that the Spekk Formation corresponds to Kimmeridgian to Berriasian “hot shales” deposited in an outer shelf environment (Norwegian Petroleum Directorate, Factpages, 2000). To the southwest, in the Slørebotn Subbasin, similar Upper Volgian to Berriasian shales were deposited as passive sediment infill (Jongenpier et al., 1996). The presence “hot shales” of Spekk Formation capping the Frøya and Gossa Highs and the Halten Terrace lead us to interpret this time as a quiescent tectonic period.

6.1.5 | Rift migration

We interpret a gradual migration of strain accommodation towards the west based on the characterisation of

the seismic sequence 2.3. This seismic sequence shows (i) the wedge-shaped geometry filling the half-graben basins generated by intra-basinal faults that offset the BCU in the western part of the supradetachment basin (Figures 5 through 7 and 13e), and (ii) the fan-shaped geometry in the immediate hanging wall of the Klakk FC and the MTFC, where fault activity was less severe to absent (Figures 5–7 and 13e). Even though rift migration during earliest Cretaceous times has been proposed in the Norwegian rifted margin (Dóre et al., 1999; Osmundsen et al., 2016; Peron-Pinvidic et al., 2013, 2018), documentation is scarce. However, migration of the deformation between three rift phases (Late Permian-Early Triassic, Late Jurassic and earliest Cretaceous) is well documented in the Viking Graben (ca. 280 km to the southwest of the study area; Bell, Jackson, Elliott, et al., 2014; Bell, Jackson, Whipp, et al., 2014). Well 6205/3-1R, in the Slørebotn Subbasin, records the only continuous sedimentation around the study area. In this well, Jongenpier et al. (1996) report conglomerates and sandstones above the Spekk Formation during the Barremian to Hauterivian, which are overlapped by Aptian Shales. On the Frøya High, biostratigraphy in wells 6306/6-1 and 6407/10-3 report an unconformity between Spekk and Lyr formations that correspond to the Valanginian to early Hauterivian times. We suggest that seismic sequence 2.3 may record the strain migration within the supradetachment basin, and may correlate with the coarse-grained deposits of the Slørebotn Subbasin and the Valanginian unconformity on the Frøya High. Some authors have suggested two rift phases in the North Atlantic rifted margin during this period: late Jurassic and earliest Cretaceous (Blystad et al., 1995; Doré et al., 1999; Peron-Pinvidic et al., 2013). Peron-Pinvidic et al. (2013) and Naliboff et al. (2017) propose that the earliest Cretaceous represent the hyperextension deformation phase, which is characterised by brittle deformation that causes low-displacement planar to listric normal faults on the thinned continental crust.

6.1.6 | Post-tectonic

We interpret seismic sequence 3.1 as post-tectonic deposits because of the observed landward steepening onlap, the ultimate burial of the Klakk FC and MTFC, and absence of growth strata in the hanging wall of the Klakk FC and MTFC (See Section 5.3.1). Overlying the proposed Spekk Formation and early Cretaceous stratigraphy, we propose that SS-3.1 may represent pre-Turonian succession equivalent to the pelagic sediments covering the Slørebotn Subbasin, Halten Terrace and Frøya High (Blystad et al., 1995 and Biostratigraphy data wells 6305/6-1 and

6305/6-2, Norwegian Petroleum Directorate, Factpages, 2000). The passive infill of the substantial accommodation in the hanging wall of the Klakk FC and MTFC is concomitant with thermal subsidence during Cretaceous and Cenozoic times. These thermal subsidence causes a tilting of the basin geometry towards the NW, change in thickness in the post-tectonic deposits (Figure 6; Bell, Jackson, Elliott, et al., 2014), which induced a “steer’s head” basin geometry (*sensu* White & Mckenzie, 1988).

6.2 | Comparison with other spoon-shaped supradetachment basins

We compare the observations of the studied basin with the main characteristics of other supradetachment basins developed in three structural configurations (Figure 1): (i) breakaway-type and spoon-like supradetachment basins within a thick continental crust (>30 km; Figure 1b,c) such as North American Cordillera (e.g., Davis, 1980), Aegean region (e.g., Jolivet et al., 2004), and Western Gneiss Region at Norway (Osmundsen et al., 1998); (ii) the breakaway-type supradetachment basin in the necking domain (Figure 1d) of the Norwegian Margin (Jongepier et al., 1996); and (iii) sag-type supradetachment basins developed in a thin continental crust (<10 km; Figure 1f) such as the Bay of Biscay and western Pyrenean (Tugend et al., 2014) and Galicia Margin (Reston et al., 2007).

The studied supradetachment basin shows a spoon-like geometry and is located between two metamorphic core complexes (Figures 1c and 4) similar to those onshore Norway for example, Hornelen, Kvamshesten and Solund supradetachment basins (Osmundsen et al., 1998; Seranne & Seguret, 1987), and in the North American Cordillera for example, the Mormon Point and Copper basins (Knott et al., 1999). The studied basin is ca. 52 km long, its width varies from ca. 30 to 50 km wide and has a maximum vertical thickness of 6 km (Section 4). These measurements are similar to the longest supradetachment basin in Norway, the Hornelen basin, which is up to 65 km long, its width varies from ca. 12 to 23 km and has a maximum vertical thickness of 10 km (Osmundsen et al., 1998; Steel et al., 1977). High-displacement, listric to low-angle normal faults exhume metamorphic core complexes (Asti et al., 2019; Cooper et al., 2010; Fillmore et al., 1994; Friedmann & Burbank, 1995; Platt et al., 2014). In the study area, these high-displacement normal faults are represented by the Klakk FC and outer strand of the MTFC, whereas the metamorphic core complexes are the Gossa High and central structural salient of the Frøya High (Figures 4–7 and Osmundsen & Péron-Pinvidic, 2018; Muñoz-Barrera et al., 2020). However, contrary to other examples of high-displacement normal faults bounding spoon-shaped

supradetachment basins, the Klakk FC and outer strand of the MTFC thinned the continental crust from ca. 26 to 11 km forming in the necking domain of the rifted margin (Figures 4–7 and Osmundsen & Péron-Pinvidic, 2018; Muñoz-Barrera et al., 2020). Osmundsen and Péron-Pinvidic (2018) and Muñoz-Barrera et al. (2020) identify a shear zone into the Gossa High and central structural salient of the Frøya High metamorphic core complexes, which we correlate with the intra-basement band of high-amplitude below the supradetachment basin (Figures 4–7). The role of the detachment or shear zones has been studied in continental core complexes (Platt et al., 2014) and exhumed subdomains of rifted margins (Lymer et al., 2019; Reston et al., 2007). Several authors propose that shear zones cause lubrication by hydrous minerals, high pore-fluid pressure, and reorientation of stress fields (Axen, 2004; Deng et al., 2017; Fossen & Cavalcante, 2017; Muñoz-Barrera et al., 2020; Osagiede et al., 2020; Wells, 2001). We interpret that shear zones below the studied basin facilitated the extension and high-displacement of the Klakk FC and outer strand of the MTFC creating the spoon-shaped supradetachment basin.

The supradetachment basin shows syn-rift post-depositional landward rotation up to ca. 37° (Figure 5) and a substantial true stratigraphic thickness of up to 30 km (Figure 6b), which is similar to that observed in other supradetachment basins for example, Hornelen, Kvamshesten and Solund, Norway (Osmundsen et al., 1998), Quantab Subbasin, Oman (Sæbø Serck et al., 2020), Slørebotn Subbasin, offshore Norway (Jongepier et al., 1996) and Galicia Margin, offshore Spain (Lymer et al., 2019). The landwards rotation of syn-tectonic strata in breakaway-type supradetachment basins reach up to 45°, for example, Slørebotn Subbasin, offshore Norway (Jongepier et al., 1996), in spoon-like supradetachment basin up to 36°, for example, Hornelen and Solund supradetachment basins, onshore Norway (Folkestad & Steel, 2001; Osmundsen et al., 1998); and in sag-type supradetachment basin up to 30° to 34°, for example, Galicia Margin, offshore Spain (Lymer et al., 2019). The restoration of section A-A' in the studied basin shows post-depositional landward rotation of the syn-tectonic deposits from horizontal at the top of seismic sequence 2.2 to ca. 37° landward at the base (Figure 5). The true stratigraphic thickness is similar also. At the Hornelen basin, only the basal part is exposed, and it shows a minimum true stratigraphic thickness up to ca. 25 km (Osmundsen et al., 1998), which correlate with the thickness observed in the studied basin. This study may complement the Ribes et al. (2019) model of syn-tectonic deposits on rifted margins, by showcasing the geometries of the succession associated with the thinning deformation phase within necking domains, which was not documented by Ribes et al. (2019).

7 | CONCLUSIONS

Based on seismic reflection, wellbore and gravity data, and using the Norwegian rifted margin as our case in point, we have, for the first time, characterised the three-dimensional structure and tectonosedimentary evolution of a spoon-shaped supradetachment basin located in the necking domain of a rifted margin. The basin evolved during a series of rift- and detachment-faulting events that eventually led to the formation of the Norwegian rifted margin. The following specific conclusions are drawn:

- This supradetachment basin has a spoon-shaped geometry with a WNW-ESE long-axis orientation, and being is ca. 53 km long and variable in width from ca. 30 km in the southeast to ca. 49 km in the northwest. Syn-tectonic deposits show landward post-depositional rotation.
- The studied basin is bounded by two high-displacement (up to 30 km), listric normal faults, the Klakk FC and the outer strand of the MTFC. These fault complexes are responsible for an observed tectonic thinning of the continental crust to ca. 11 km beneath the supradetachment basin, compared with a crustal thickness of ca. 27 km in the proximal domain. Consequently, these faults formed the necking domain of the Norwegian rifted margin in this area.
- The studied spoon-shaped supradetachment basin is located between two continental margin core complexes that sit in their footwall of the bounding faults, namely the Frøya High and Gossa Highs. These metamorphic core complexes show high positive gravity anomalies with oval geometries that may represent rocks of the middle to lower continental crust (Muñoz et al., 2020; Osmundsen & Péron-Pinvidic, 2018; Slagstad et al., 2011)
- The low-angle detachment parts of the bounding Klakk FC and MTFC show a relationship with pre-existing shear zones (The Sløreboth detachment continuing westward off the Gossa High, see Osmundsen & Péron-Pinvidic, 2018) and the SF4 shear zone (Continuing westward of the Frøya High described by Muñoz et al., 2020), whereby they merge onto these shear zones at ca. 12 km depth.
- The Jan Mayen lineament does not connect to the Klakk FC or MTFC. Instead, it dies out to the northwest part of the supradetachment basin forming intra-basinal normal faults.
- This part of the Norwegian margin shows a “steer-head basin geometry, which is filled by three seismic megasequences: a pre-tectonic (seismic megasequence 1), a syn-tectonic (seismic megasequence 2) and a post-tectonic (seismic megasequence 3). Our structural restoration shows that the entire basin is tilted towards the northwest due to post-rift thermal subsidence.
- The syn-tectonic succession within the supradetachment basin (Megasequence 2) is up to 30 km thick (true stratigraphic thickness), recording deposition during two rift episodes (inferred late Jurassic and earliest Cretaceous, respectively, based on known regional events) separated by a short quiescent tectonic period. The early rift episode includes the seismic sequence 2.1 and 2.2, while seismic sequence 2.3 represents the later rift episode.
- The initiation stage of the early rift episode succession preserves Gilbert delta deposits with large foreset highs (seismic sequence 2.1), which we interpret as reflecting onset of faulting likely during Bathonian to early Oxfordian times. Subsequently, during the rift climax, the area is overlaid by a thick (up to 23 km) sedimentary wedge (seismic sequence 2.2), which we interpret to record a stage of strain localisation and maximum fault activity presumably during the Oxfordian to Kimmeridgian times.
- The syn-tectonic succession of the early (late Jurassic) rift episode is capped by a high amplitude continuous reflections, which we interpret to reflect fine-grained pelagic deposits (shales) deposited during a quiescent tectonic period surely during Kimmeridgian to Berriasian times.
- The supradetachment basin recorded the basin-ward migration of rifting during the later rift episode (likely Valanginian-early Hauterivian), which is supported by: (i) Intra-basinal faults dissected the intra-rift pelagics deposits, creating wedge-shaped basins in the western part of the supradetachment basin, and (ii) the fault activity recorded along the Klakk FC and MTFC were less expressed during this time compared with the early rift episode.
- The spoon-shaped supradetachment basin (studied here), and the breakaway-type Slørebotn Subbasin supradetachment basin (Osmundsen & Péron-Pinvidic, 2018) are located in a necking domain of a rifted margin with a thick continental crust (>26 km). Similar basins are likely to exist in the necking domain of other margins; the integration of deep seismic reflection data with gravity anomaly data may allow the identification and characterisation of such similar supradetachment basins at rifted margins globally.

ACKNOWLEDGEMENTS

This contribution forms part of the Syn-Rift Systems Project funded by the Research Council of Norway (project number 255229) and a consortium of industry partners, including, Aker BP, ConocoPhillips, DNO, Equinor, Neptune and Tullow Oil. We are grateful to our academic project partners, universities of Leeds, East Anglia,

Lorraine and to the National and Kapodistrian University of Athens. We thank Diskos, Tullow Oil and TGS for the access to reflection seismic and wellbore data, and for granting the permissions necessary to publish selected images of said data in the present manuscript. Schlumberger and Petroleum Experts are gratefully acknowledged for access to academic licenses to Petrel and Move software. We thank Yuriy Maystrenko for access to Moho depth data. David Peacock, Johannes Wiest, Leo Zijerveld and Tim Cullen are thanked for discussions and comments on the manuscript. Finally, we thank Tony Doré, Per Terje Osmundsen, one anonymous reviewer, and Editor Zoë Mildon, whose insightful comments and suggestions led to significant improvements to this paper.

CONFLICT OF INTEREST

There are no conflicts of interest to declare.

PEER REVIEW

The peer review history for this article is available at <https://publons.com/publon/10.1111/bre.12648>.

DATA AVAILABILITY STATEMENT

The data used for this research are confidential industry seismic reflections and well data and cannot be shared.

ORCID

Jhon M. Muñoz-Barrera  <https://orcid.org/0000-0001-6802-1623>

Atle Rotevatn  <https://orcid.org/0000-0002-8413-3294>

Robert L. Gawthorpe  <https://orcid.org/0000-0002-4352-6366>

Gijs Henstra  <https://orcid.org/0000-0001-9805-5875>

Thomas B. Kristensen  <https://orcid.org/0000-0003-0658-8012>

REFERENCES

- Andersen, T. B., & Jamtveit, B. (1990). Uplift of deep crust during orogenic extensional collapse: A model based on field studies in the Sogn-Sunnfjord region of western Norway. *Tectonics*, 9(5), 1097–1111. <https://doi.org/10.1029/TC009i005p01097>
- Asti, R., Faccena, C., Rossetti, F., Malusà, M. G., Gliozzi, E., Faranda, C., Lirer, F., & Cosentino, D. (2019). The Gediz supradetachment system (SW Turkey): Magmatism, tectonics, and sedimentation during crustal extension. *Tectonics*, 38, 1414–1440. <https://doi.org/10.1029/2018TC005181>
- Asti, R., Malusà, M. G., & Faccena, C. (2018). Supradetachment basin evolution unravelled by detritalapatite fission track analysis: The Gediz Graben (Menderesmassif, Western Turkey). *Basin Research*, 30, 502–521. <https://doi.org/10.1111/bre.12262>
- Axen, G. J. (2004). Mechanics of low-angle normal faults, Chapter 3. In G. D. Karner, B. Taylor, N. W. Driscoll, & D. J. Kohlstedt (Eds.), *Rheology and deformation of the lithosphere at continental margins* (pp. 46–91). Columbia University Press.
- Bell, R., Jackson, C., Elliott, G., Gawthorpe, R., Sharp, I. R., & Michelsen, L. (2014). Insights into the development of major rift-related unconformities from geologically constrained subsidence modelling: Halten terrace, Offshore Mid Norway. *Basin Research*, 26, 203–224. <https://doi.org/10.1111/bre.12049>
- Bell, R., Jackson, C.-A.-L., Whipp, P. S., & Clements, B. (2014). Strain migration during multiphase extension: Observations from the northern North Sea. *Tectonics*, 33, 1936–1963. <https://doi.org/10.1002/2014TC003551>
- Blystad, P., Brekke, H., & Faereth, R. B. (1995). *Structural elements of the Norwegian continental shelf. Pt. 2. The Norwegian Sea Region*. Norwegian Petroleum Directorate.
- Braathen, A., Nordgulen, Ø., Osmundsen, P. T., Andersen, T. B., Solli, A., & Roberts, D. (2000). Devonian, orogen-parallel, opposed extension in the Central Norwegian Caledonides. *Geology*, 28, 615–618. [https://doi.org/10.1130/0091-7613\(2000\)28<615:DOOEIT>2.0.CO;2](https://doi.org/10.1130/0091-7613(2000)28<615:DOOEIT>2.0.CO;2)
- Bukta, K. E. (2018). *Slørebotn sub-basin tectono-stratigraphic framework* (Master thesis). University of Stavanger. <https://uis.brage.unit.no/uis-xmlui/handle/11250/2563002>
- Chéry, J. (2001). Core complex mechanics: From the gulf of corinth to the snake range. *Geology*, 29, 439–442. [https://doi.org/10.1130/0091-7613\(2001\)029<0439:CCMFTG>2.0.CO;2](https://doi.org/10.1130/0091-7613(2001)029<0439:CCMFTG>2.0.CO;2)
- Chiarella, D., Capella, W., Longhitano, S. G., & Muto, F. (2020). Fault-controlled base-of-scarp deposits. *Basin Research*, 33(2), 1056–1075. <https://doi.org/10.1111/bre.12505>
- Chiarella, D., Longhitano, S. G., Mosdell, W., & Telesca, D. (2020). Sedimentology and facies analysis of ancient sand ridges: Jurassic Rogn formation, Trøndelag platform, offshore Norway. *Marine and Petroleum Geology*, 112, 104082. <https://doi.org/10.1016/j.marpetgeo.2019.104082>
- Cooper, F. J., Platt, J. P., Anczkiewica, R., & Whitehouse, M. J. (2010). Footwall dip of a core complex detachment fault: Thermobarometric constraints from the Northern Snake range (Basin and Range, USA). *Journal of Metamorphic Geology*, 28, 997–1020. <https://doi.org/10.1111/j.1525-1314.2010.00907.x>
- Corfu, F., Andersen, T. B., & Gasser, D. (2014). The Scandinavian Caledonides: Main features, conceptual advances and critical questions. *Geological Society*, 390, 9–43. <https://doi.org/10.1144/SP390.25>
- Dalland, A., Worsley, D., & Ofstad, K. (1988). *A Lithostratigraphic scheme for the mesozoic and cenozoic and succession offshore mid- and northern Norway*. Oljedirektoratet.
- Davis, G. H. (1980). Structural characteristics of metamorphic core complexes, Southern Arizona. In M. D. Crittenden, P. J. Coney, & G. H. Davis (Eds.), *Cordilleran metamorphic core complexes, memoir* (Vol. 153, pp. 35–77). The Geological Society of America.
- Deng, C., Gawthorpe, R. L., Finch, E., & Fossen, H. (2017). Influence of a pre-existing basement weakness on normal fault growth during oblique extension: Insights from discrete element modeling. *Journal of Structural Geology*, 105, 44–61. <https://doi.org/10.1016/j.jsg.2017.11.005>
- Dermircioğlu, D., Ecevitoglu, E., & Seyitoğlu, G. (2010). Evidence of a rolling hinge mechanism in the seismic records of the hydrocarbon-bearing Alaşehir Graben, Western Turkey. *Petroleum Geoscience*, 16, 155–160. <https://doi.org/10.1144/1354-079309-017>
- Doré, A., Lundin, E., Jensen, L., Birkeland, Ø., Eliassen, P., & Fichler, C. (1999). Principal tectonic events in the evolution of

- the Northwest European Atlantic margin. In A. J. Fleet, A. J. Fleet, & S. A. R. Boldy (Eds.), *Petroleum geology of Northwest Europe: Proceedings of the 5th Conference* (Vol. 5, pp. 41–61). Petroleum Geology Conference Series, Geological Society of London. <https://doi.org/10.1144/0050041>
- Ebbing, J., & Olesen, O. (2011). New compilation of top basement and basement thickness for the norwegian continental shelf reveals the segmentation of the passive margin system. In B. A. Vining & S. C. Pickering (Eds.), *Petroleum geology: From mature basins to new frontiers - Proceedings of the 7th Petroleum Geology Conference* (pp. 885–897). The Geological Society. <https://doi.org/10.1144/0070885>
- Elliott, G. M., Jackson, C. A. L., Gawthorpe, R. L., Wilson, P., Sharp, I. R., & Michelsen, L. (2015). Late Syn-Rift evolution of the Vingleia fault complex, Halten terrace, offshore Mid-Norway; a test of rift basin tectono-stratigraphic models. *Basin Research*, 1–23. <https://doi.org/10.1111/bre.12158>
- Faleide, J. I., Tsikalas, F., Breivik, A. J., Mjelde, R., Ritzmann, O., Engen, O., Wilson, J., & Eldholm, O. (2008). Structure and evolution of the continental margin off Norway and the Barents sea. *Episodes*, 31, 82–91. <https://doi.org/10.18814/epiugs/2008/v31i1/012>
- Fillmore, R. P., Walker, J. D., Bartley, J. M., & Glazner, A. F. (1994). Development of three genetically related basins associated with detachment-style faulting: Predicted characteristics and an example from the Central Mojave Desert, California. *Geology*, 88, 1087–1090. [https://doi.org/10.1130/0091-7613\(1994\)022<1087:DOTGRB>2.3.CO;2](https://doi.org/10.1130/0091-7613(1994)022<1087:DOTGRB>2.3.CO;2)
- Folkestad, A., & Steel, R. J. (2001). The alluvial cyclicity in hornelen basin (devonian Western Norway) revisited: A multiparameter sedimentary analysis and stratigraphic implications. In O. J. Martinsen & T. Dreyer (Eds.), *Sedimentary environments offshore Norway – Palaeozoic to recent, NPF Special Publication* (Vol. 10, pp. 39–50). Norwegian Petroleum Society. [https://doi.org/10.1016/S0928-8937\(01\)80007-2](https://doi.org/10.1016/S0928-8937(01)80007-2)
- Ford, M., Rohais, S., Williams, E. A., Bourlange, S., Jousselin, D., Backert, N., & Malartre, F. (2013). Tectono-sedimentary evolution of the Western Corinth Rift (Central Greece). *Basin Research*, 25, 3–25. <https://doi.org/10.1111/j.1365-2117.2012.00550.x>
- Forshee, E. J., & Yin, A. (1995). Evolution of monolithological breccia deposits in supradetachment basins, Whipple Mountains, California. *Basin Research*, 7, 181–197. <https://doi.org/10.1111/j.1365-2117.1995.tb00103.x>
- Fossen, H. (2010). Extensional tectonics in the North Atlantic Caledonides: A regional view. *Geological Society, Special Publications*, 335, 767–793. <https://doi.org/10.1144/SP335.31>
- Fossen, H., & Cavalcante, G. C. (2017). Shear zones – A review. *Earth-Science Reviews*, 171, 434–455. <https://doi.org/10.1016/j.earscirev.2017.05.002>
- Friedmann, S. J., & Burbank, D. W. (1995). Rift basins and supradetachment basins: Intracontinental extensional end-members. *Basin Research*, 7, 109–127. <https://doi.org/10.1111/j.1365-2117.1995.tb00099.x>
- Gabrielsen, R. H., Odinsen, T., & Grunnaleite, I. (1999). Structuring of the Northern Viking Graben and the Møre basin; the influence of basement structural grain, and the particular role of the Møre-Trøndelag fault complex. *Marine and Petroleum Geology*, 16, 443–465. [https://doi.org/10.1016/S0264-8172\(99\)00006-9](https://doi.org/10.1016/S0264-8172(99)00006-9)
- Gawthorpe, R., Fraser, A. J., & Collier, R. E. L. (1994). Sequence stratigraphy in active extensional basins: Implications for the interpretation of ancient basin-fills. *Marine and Petroleum Geology*, 11, 642–658. [https://doi.org/10.1016/0264-8172\(94\)90021-3](https://doi.org/10.1016/0264-8172(94)90021-3)
- Gee, D. G., Janák, M., Majka, J., Robinson, P., & van Roermund, H. (2013). Subduction along and within the Baltoscandian margin during closing of the Iapetus Ocean and Baltica-Laurentia collision. *Lithosphere*, 5(2), 169–178. <https://doi.org/10.1130/L220.1>
- Gernigon, L., Franke, D., Geoffroy, L., Schiffer, C., Foulger, G. R., & Stoker, M. S. (2020). Crustal fragmentation, magmatism, and the diachronous opening of the Norwegian-Greenland sea. In C. Doglioni (Ed.), *A new paradigm for the North Atlantic realm, earth-science reviews* (Vol. 206, 37 pp). <https://doi.org/10.1016/j.earscirev.2019.04.011>
- Gernigon, L., Olesen, O., Ebbing, J., Wienecke, S., Gaina, C., Mogaard, J. O., Sand, M., & Myklebust, R. (2009). Geophysical insights and early spreading history in the vicinity of the Jan Mayen fracture zone, Norwegian-Greenland sea. *Tectonophysics*, 468, 185–205. <https://doi.org/10.1016/j.tecto.2008.04.025>
- Groshong, R. H. J. (2006). *3D structural geology: A practical guide to quantitative surface and subsurface map interpretation*. Springer.
- Hubbard, R. J. (1988). Age and significance of sequence boundaries on Jurassic and early Cretaceous rifted continental margins. *AAPG Bulletin*, 72(1), 49–72. <https://doi.org/10.1306/703C81C8-1707-11D7-8645000102C1865D>
- Jolivet, L., Famin, V., Mehl, C., Parra, T., Aubourg, C., Hébert, R., & Philippot, P. (2004). Strain localization during crustal-scale boudinage to form extensional metamorphic domes in the Aegean sea. In D. L. Whitney, C. Teyssier, & C. S. Siddoway (Eds.), *Gneiss domes in Orogeny, Special Paper* (Vol. 380, pp. 185–210). Geological Society of America. <https://doi.org/10.1130/0-8137-2380-9.185>
- Jones, G., Welbon, A., Mohammadlou, H., Sakharov, A., Ford, J., Needham, T., & Ottesen, C. (2020). Complex stratigraphic fill of a small, confined syn-rift basins: And Upper Jurassic example from offshore Mid-Norway. In D. Chiarella, S. G. Archer, J. A. Howell, C.-A.-L. Jackson, H. Kombrink, & S. Patruno (Eds.), *Cross-border themes in petroleum geology II: Atlantic margin and Barents sea, Special Publication* (Vol. 495, 39 pp). Geological Society. <https://doi.org/10.1144/SP495-2019-143>
- Jongepier, K., Cecilie, J., & Grue, K. (1996). Triassic to early cretaceous stratigraphic and structural development of the Northeastern Møre Basin margin, off Mid-Norway. *Norsk Geologisk Tidsskrift*, 76, 199–214.
- Kapp, P., Taylor, M., Stockli, D., & Ding, L. (2008). Development of active low-angle normal fault systems during orogenic collapse: Insight from Tibet. *Geology*, 36, 7–10. <https://doi.org/10.1130/G24054A.1>
- Knott, J. R., Sarna-Wojcicki, A. M., Meyer, C. E., Tinsley, J. C., III, Wells, S. G., & Wan, E. (1999). Late cenozoic stratigraphic and tephrochronology of the western Black Mountains piedmont, Death Valley, California: Implications for the tectonic development of Death Valley. In L. A. Wright & B. W. Troxel (Eds.), *Cenozoic basins of the Death Valley Region, GSA Special papers* (Vol. 333, pp. 345–366). The Geological Society of America. <https://doi.org/10.1130/0-8137-2333-7.345>
- Lister, G. S., Etheridge, M. A., & Symonds, P. A. (1986). Detachment faulting and the evolution of passive continental margins. *Geology*, 14, 246–250. <https://doi.org/10.1016/j.marpetgeo.2013.02.002>

- Lymer, G., Cresswell, D. J. F., Reston, T. J., Bull, J. M., Sawyer, D. S., Morgan, J. K., Stevenson, C., Causer, A., Minshull, T. A., & Shillington, D. J. (2019). 3D development of detachment faulting during continental breakup. *Earth and Planetary Science Letters*, *515*, 90–99. <https://doi.org/10.1016/j.epsl.2019.03.018>
- Masini, E., Manatschal, G., Mohn, G., & Unternehr, P. (2012). Anatomy and tectono-sedimentary evolution of a rift-related detachment system: The example of the err detachment (Central Alps, Se Switzerland). *GSA Bulletin*, *124*, 1535–1551. <https://doi.org/10.1130/B30557.1>
- Maystrenko, Y., Gernigon, L., Nasuti, A., & Olesen, O. (2018). Deep structure of the mid-Norwegian continental margin (the Vøring and Møre Basins) according to 3-D density and magnetic modelling. *Geophysical Journal International*, *212*, 1696–1721. <https://doi.org/10.1093/gji/ggx491>
- McCloughry, J. D., & Gaylord, D. R. (2005). Middle eocene sedimentary and volcanic infilling of an evolving Supradetachment basin: White Lake Basin, South-Central British Columbia. *Canadian Journal of Earth Sciences*, *42*, 49–66. <https://doi.org/10.1139/e04-105>
- Miller, M. B., & Pavlis, T. L. (2005). The black mountains turtlebacks: Rosetta stones of death valley tectonics. *Earth-Science Reviews*, *73*, 115–138. <https://doi.org/10.1016/j.earscirev.2005.04.007>
- Mjelde, R., Faleide, J. I., Breivik, A. J., & Raum, T. (2009). Lower crustal composition and crustal lineaments on the Vøring Margin, Ne Atlantic: A review. *Tectonophysics*, *472*, 183–193. <https://doi.org/10.1016/j.tecto.2008.04.018>
- Mjelde, R., Goncharov, A., & Müller, R. (2013). The Moho: Boundary above upper mantle peridotites or lower crustal Eclogites? A global review and new interpretations for passive margins. *Tectonophysics*, *609*, 636–650. <https://doi.org/10.1016/j.tecto.2012.03.001>
- Mjelde, R., Kvarven, T., Faleide, J. I., & Thybo, H. (2016). Lower crustal high-velocity bodies along North Atlantic passive margins, and their link to Caledonian suture zone eclogites and early cenozoic magmatism. *Tectonophysics*, *670*, 16–29. <https://doi.org/10.1016/j.tecto.2015.11.021>
- Mørk, M. B., & Johnsen, S. O. (2005). Jurassic sandstone provenance and basement erosion in the Møre margin – Froan basin area. *NGU Bulletin*, *443*, 5–18.
- Mørk, M. B., & Stiberg, J.-P. (2003). Basement erosion and Mesozoic sandstone provenance in the Møre margin area: Extended abstract. In *Petroleum exploration and production in environmentally sensitive areas* (pp. 41–44). Norwegian Petroleum Society.
- Müller, R., Nystuen, J. P., Eide, F., & Lie, H. (2005). Late permian to Triassic basin infill history and palaeogeography of the mid-Norwegian shelf – East Greenland region. In B. Wandas (Ed.), *Onshore-offshore relationships on the North Atlantic Margin, Special Publication* (Vol. 12, pp. 165–189). Norwegian Petroleum Society. [https://doi.org/10.1016/S0928-8937\(05\)80048-7](https://doi.org/10.1016/S0928-8937(05)80048-7)
- Muñoz-Barrera, J. M., Henstra, G. A., Kristensen, T., Gawthorpe, R., & Rotevatn, A. (2020). The role of structural inheritance in the development of high-displacement crustal faults in the necking domain of rifted margins: The Klakk fault complex, Frøya high, offshore mid-Norway. *Journal of Structural Geology*, *140*, 104163. <https://doi.org/10.1016/j.jsg.2020.104163>
- Naliboff, J. B., Buitter, S. J. H., Péron-Pinvidic, G., Osmundsen, P. T., & Tetreault, J. (2017). Complex fault interaction controls continental rifting. *Nature Communications*, *8*, 1–9. <https://doi.org/10.1038/s41467-017-00904-x>
- Nasuti, A., Pascal, C., & Ebbing, J. (2012). Onshore-offshore potential field analysis of the Møre-Trøndelag fault complex and adjacent structures of mid Norway. *Tectonophysics*, *518–521*, 17–28. <https://doi.org/10.1016/j.tecto.2011.11.003>
- Norwegian Petroleum Directorate, Factpages. (2000). *Norwegian Petroleum Directorate*. <https://factpages.npd.no/en/wellbore/PageView/Exploration/All>
- Olesen, O., Ebbing, J., Gellein, J., Kihle, O., Myklebust, R., Sand, M., Skilbrei, J. R., Solheim, D., & Usov, S. (2010). *Gravity anomaly map, Norway and adjacent areas*. Geological Survey of Norway. <https://www.ngu.no/en/publikasjon/gravity-anomaly-map-norway-and-adjacent-areas-scale-13-mill>
- Olesen, O., Gellein, J., Gernigon, L., Kihle, O., Koziel, J., Lauritsen, T., Mogaard, J. O., Myklebust, R., Skilbrei, J. R., & Usov, S. (2010). *Magnetic anomaly map, Norway and adjacent areas*. Geological Survey of Norway. <https://www.ngu.no/en/publikasjon/magnetic-anomaly-map-norway-and-adjacent-areas-scale-13-mill>
- Osagiede, E., Rotevatn, A., Gawthorpe, R. L., Kristensen, T., Jackson, C.-A.-L., & Marsh, N. (2020). Pre-existing intra-basement shear zones influence growth and geometry of non-colinear normal faults, Western Utsira High-Heimdal terrace, North Sea. *Journal of Structural Geology*, *130*, 103908. <https://doi.org/10.1016/j.jsg.2019.103908>
- Osmundsen, P. T., & Andersen, T. B. (2001). The middle Devonian basins of Western Norway: Sedimentary response to large transtensional tectonics? *Tectonophysics*, *332*, 51–68. [https://doi.org/10.1016/S0040-1951\(00\)00249-3](https://doi.org/10.1016/S0040-1951(00)00249-3)
- Osmundsen, P. T., Andersen, T. B., Markussen, S., & Svendby, A. K. (1998). Tectonics and sedimentation in the Hangingwall of a major extensional detachment: The Devonian Kvamshesten basin, Western Norway. *Basin Research*, *10*, 213–234. <https://doi.org/10.1046/j.1365-2117.1998.00064.x>
- Osmundsen, P. T., Braathen, A., Sommaruga, A., Skilbrei, J. R., Nordgulen, Ø., Roberts, D., Andersen, T. B., Olesen, O., & Mosar, J. (2005). Metamorphic core complexes and gneiss-cored culminations along the Mid-Norwegian Margin: An overview and some current ideas. In B. Wandas, J. P. Nystuen, E. Eide, & F. M. Gradstein (Eds.), *Onshore-offshore relationships on the North Atlantic Margin* (Vol. 12, pp. 29–41). Norwegian Geological Society. [https://doi.org/10.1016/S0928-8937\(05\)80042-6](https://doi.org/10.1016/S0928-8937(05)80042-6)
- Osmundsen, P. T., & Péron-Pinvidic, G. (2018). Crustal scale fault interaction at rifted margins and the formation of domain-bounding breakaway complexes: Insights from offshore Norway. *Tectonics*, *37*, 935–964. <https://doi.org/10.1002/2017TC004792>
- Osmundsen, P. T., Péron-Pinvidic, G., & Bunkholt, H. (2021). Rifting of collapsed orogens: Successive incision of continental crust in the proximal margin offshore Norway. *Tectonics*, *40*, e2020TC006283. <https://doi.org/10.1029/2020TC006283>
- Osmundsen, P. T., Péron-Pinvidic, G., Ebbing, J., Erratt, D., Fjellanger, E., Bergslien, D., & Syvertsen, S. E. (2016). Extension, hyperextension and mantle exhumation offshore Norway: A discussion based on 6 crustal transects. *Norwegian Journal of Geology*, *96*, 343–372. <https://doi.org/10.17850/njg96-4-05>
- Pechlivanidou, S., Cowie, P. A., Hannisdal, B., Whittaker, A., Gawthorpe, R., Pennos, C., & Riiser, O. S. (2018). Source-to-sink analysis in an active extensional setting: Holocene erosion and deposition in the Sperchios Rift, Central Greece. *Basin Research*, *30*, 522–543. <https://doi.org/10.1111/bre.12263>
- Peron-Pinvidic, G., Manatschal, G., & Osmundsen, P. T. (2013). Structural comparison of archetypal Atlantic rifted margins: A review of

- observations and concepts. *Marine and Petroleum Geology*, 43, 21–47. <https://doi.org/10.1016/j.marpetgeo.2013.02.002>
- Péron-Pinvidic, G., & Osmundsen, P. T. (2018). The Mid Norwegian – NE Greenland conjugate margins: Rifting evolution, margin segmentation, and breakup. *Marine and Petroleum Geology*, 98, 162–184. <https://doi.org/10.1016/j.marpetgeo.2018.0011>
- Peron-Pinvidic, G., Osmundsen, P. T., & Bunkholt, H. (2020). The proximal domain of the Mid-Norwegian rifted margin: The Trøndelag platform revisited. *Tectonophysics*, 790, 228551. <https://doi.org/10.1016/j.tecto.2020.228551>
- Platt, J. P., Behr, W. M., & Cooper, F. J. (2014). Metamorphic core complexes: Windows into the mechanics and reology of the crust. *Journal of the Geological Society*, 172, 9–27. <https://doi.org/10.1144/jgs2014-036>
- Prosser, S. (1993). Rift-related linked depositional systems and their seismic expression. In G. D. Williams & A. Dobb (Eds.), *Tectonics and seismic sequence stratigraphy, Special Publications* (pp. 35–66). Geological Society. <https://doi.org/10.1144/GSL.SP.1993.071.01.03>
- Provan, D. M. (1992). Draugen oil field, Haltenbanken Province, Offshore Norway. In M. T. Halbouty (Ed.), *Giant oil and gas fields of the decade 1978–1988, AAPG Memoir* (Vol. 54, pp. 371–382). AAPG.
- Ravnås, R., Berge, K., Campbell, H., Harvey, C., & Norton, M. J. (2014). Halten terrace lower and middle Jurassic inter-rift megasequence analysis: Megasequence structure, sedimentary architecture and controlling parameters. In A. W. Martinius, R. Ravnås, R. J. Steel, & J. P. Wonham (Eds.), *From depositional systems to sedimentary successions on the Norwegian Continental Margin, Special Publications* (pp. 215–251). Wiley Blackwell. <https://doi.org/10.1002/9781118920435.ch10>
- Redfield, T. F., Braathen, A., Gabrielsen, R., Osmundsen, P. T., Torsvik, T. H., & Andriessen, P. A. M. (2005). Late mesozoic to early cenozoic components of vertical separation across the Møre-Trøndelag fault complex, Norway. *Tectonophysics*, 395, 233–249. <https://doi.org/10.1016/j.tecto.2004.09.012>
- Reston, T. J., Leytheuser, T., Booth-Rea, G., Sawyer, D., Klaeschen, D., & Long, C. (2007). Movement along a low-angle normal fault: The S reflector west of Spain. *Geochemistry, Geophysics, Geosystems*, 8(6), 1–14. <https://doi.org/10.1029/2006GC001437>
- Ribes, C., Ghienne, J.-F., Manatschal, G., Decarli, A., Karner, G. D., Figueredo, P. H., & Johnson, C. A. (2019). Long-lived mega fault-scarps and related Breccias at distal rifted margins: Insights from present-day and fossil analogues. *Journal of the Geological Society*, 176, 801–816. <https://doi.org/10.1144/jgs2018-181>
- Rohais, S., Eschard, R., Ford, M., Guillocheau, F., & Moretti, I. (2007). Stratigraphic Architecture of the Plio-Pleistocene infill of the Corinth Rift: Implications for its structural evolution. *Tectonophysics*, 440, 5–28. <https://doi.org/10.1016/j.tecto.2006.11.006>
- Sæbø Serck, C., Braathen, A., Olausson, S., Osmundsen, P. T., Midtkandal, I., van Yperen, A. E., & Indrevar, K. (2020). Supradetachment to rift basin transition recorded in continental to marine deposition; Paleogene Bandar Jissah Basin, Ne Oman. *Basin Research*, 33(1), 544–569. <https://doi.org/10.1111/bre.12484>
- Sangree, J. B., & Widmier, J. M. (1979). Interpretation of depositional facies from seismic data. *Geophysics*, 44, 131–160. <https://doi.org/10.1190/1.1440957>
- Seranne, M., & Seguret, M. (1987). The Devonian basins of Western Norway: Tectonics and kinematics of an extending crust. In M. P. Coward, J. F. Dewey, & P. L. Hancock (Eds.), *Continental extensional tectonics, Special Publication* (Vol. 28, pp. 537–548). Geological Society. <https://doi.org/10.1144/GSL.SP.1987.028.01.35>
- Slagstad, T., Davidsen, B., & Daly, J. S. (2011). Age and composition of crystalline basement rocks on the Norwegian continental margin: Offshore extension and continuity of the Caledonian–Appalachian orogenic belt. *Journal of the Geological Society*, 168, 1167–1185. <https://doi.org/10.1144/0016-76492010-136>
- Sommaruga, A., & Bøe, R. (2002). Geometry and Subcrop maps of shallow Jurassic basins along the mid-Norwegian coast. *Marine and Petroleum Geology*, 19, 1029–1042. [https://doi.org/10.1016/S0264-8172\(02\)00113-7](https://doi.org/10.1016/S0264-8172(02)00113-7)
- Steel, R. J., Mæhle, S., Nilsen, H., Røe, S. L., & Spinnangr, Å. (1977). Coarsening-upward cycles in the alluvium of Homeien Basin (Devonian) Norway: Sedimentary response to tectonic events. *Geological Society of America Bulletin*, 88, 1124–1134.
- Trice, R., Hiorth, C., & Holdsworth, R. (2019). Fractured basement play development on the UK and Norwegian Rifted margins. In D. Chiarella, S. G. Archer, J. A. Howell, C.-A.-L. Jackson, H. Kombrink, & S. Patruno (Eds.), *Cross-border themes in petroleum Geology II: Atlantic margin and Barents Sea, Special Publications* (Vol. 495, 25 pp). Geological Society. <https://doi.org/10.1144/SP495-2018-174>
- Tsikalas, F., Faleide, J. I., Eldholm, O., & Blaich, O. A. (2012). The NE Atlantic conjugate margins. In D. G. Roberts & A. W. Bally (Eds.), *Phanerozoic passive margins, Cratonic basins and global tectonic maps* (Vol. 5, pp. 141–201). Elsevier.
- Tugend, J., Manatschal, G., Kusznir, N. J., & Masini, E. (2014). Characterizing and identifying structural domains at rifted continental margins: Application to the Bay of Biscay margins and Its Western Pyrenean Fossil remnants. In G. M. Gibson, F. Roure, & G. Manatschal (Eds.), *sedimentary basins and crustal processes at continental margins: From modern hyper-extended margins to deformed ancient analogues, Special Publications* (Vol. 413, pp. 171–203). Geological Society. <https://doi.org/10.1144/SP413.3>
- Vetti, V., & Fossen, H. (2012). Origin of contrasting Devonian supradetachment basin types in the Scandinavian Caledonides. *Geology*, 40, 571–574. <https://doi.org/10.1130/G32512.1>
- Wells, M. L. (2001). Rheological control on the initial geometry of the raft river detachment fault and shear zone, Western United States. *Tectonics*, 20, 435–457. <https://doi.org/10.1029/2000TC001202>
- Wernicke, B. (1981). Low-angle normal faults in the Basin and Range Province: Nappe tectonics in an extending orogen. *Nature*, 291, 645–648. <https://doi.org/10.1038/291645a0>
- White, N., & McKenzie, D. (1988). Formation of the “steer’s head” geometry of sedimentary basins by differential stretching of the crust and mantle. *Geology*, 16, 250–253. [https://doi.org/10.1130/0091-7613\(1988\)016<0250:FOTSSH>2.3.CO;2](https://doi.org/10.1130/0091-7613(1988)016<0250:FOTSSH>2.3.CO;2)
- Whitney, D. L., Teyssier, C., Rey, P., & Buck, W. R. (2013). Continental and oceanic core complexes. *Geological Society of America Bulletin*, 125, 273–298. <https://doi.org/10.1130/B30754.1>
- Wiest, J. D., Osmundsen, P. T., Jacobs, J., & Fossen, H. (2019). Deep crustal flow within post-orogenic metamorphic core complexes – Insights 1 from the Southern Western Gneiss region of Norway. *Tectonics*, 38, 4267–4289. <https://doi.org/10.1029/2019TC005708>
- Wilson, P., Elliott, G. M., Gawthorpe, R. L., Jackson, C.-A.-L., Michelsen, L., & Sharp, I. R. (2013). Geometry and segmentation of an evaporite-detached normal fault array: 3D seismic analysis of the Southern Bremstein fault complex, Offshore

Mid-Norway. *Journal of Structural Geology*, 51, 74–91. <https://doi.org/10.1016/j.jsg.2013.03.005>

Wilson, P., Elliott, G. M., Gawthorpe, R. L., Jackson, C. A., Michelsen, L., & Sharp, I. R. (2015). Lateral variation in structural style along an evaporite-influenced rift fault system in the Halten Terrace, Norway: Influence of basement structure and evaporite facies. *Journal of Structural Geology*, 79, 110–123. <https://doi.org/10.1016/j.jsg.2015.08.002>

Woodruff, W. H. J., Horton, B. K., Kapp, P., & Stockli, D. (2013). Late Cenozoic evolution of the Lunggar extensional Basin, Tibet: Implications for basin growth and exhumation in Hinterland Plateaus. *GSA Bulletin*, 125, 343–358. <https://doi.org/10.1130/B30664.1>

Zastrozhnov, D., Gernigon, L., Godin, I., Abdelmalak, M. M., Planke, S., Faleide, J. I., Eide, S., & Myklebust, R. (2018). Cretaceous-paleocene evolution and crustal structure of the Northern Vøring Margin (Offshore Mid-Norway): Results from

integrated geological and geophysical study. *Tectonics*, 37, 497–528. <https://doi.org/10.1002/2017TC004655>

SUPPORTING INFORMATION

Additional supporting information may be found in the online version of the article at the publisher's website.

How to cite this article: Muñoz-Barrera, J. M., Rotevatn, A., Gawthorpe, R. L., Henstra, G., & Kristensen, T. B. (2022). Supradetachment basins in necking domains of rifted margins: Insights from the Norwegian Sea. *Basin Research*, 00, 1–29. <https://doi.org/10.1111/bre.12648>